

Alma Mater Studiorum Università di Bologna
Archivio istituzionale della ricerca

Role of the (pseudo)halido ligand in ruthenium(ii): p -cymene a-amino acid complexes in speciation, protein reactivity and cytotoxicity

This is the final peer-reviewed author's accepted manuscript (postprint) of the following publication:

Published Version:

Biancalana L., Zanda E., Hadiji M., Zacchini S., Pratesi A., Pampaloni G., et al. (2021). Role of the (pseudo)halido ligand in ruthenium(ii): p -cymene a-amino acid complexes in speciation, protein reactivity and cytotoxicity. DALTON TRANSACTIONS, 50, 15760-15777 [10.1039/d1dt03274g].

Availability:

This version is available at: <https://hdl.handle.net/11585/851697> since: 2023-06-09

Published:

DOI: <http://doi.org/10.1039/d1dt03274g>

Terms of use:

Some rights reserved. The terms and conditions for the reuse of this version of the manuscript are specified in the publishing policy. For all terms of use and more information see the publisher's website.

This item was downloaded from IRIS Università di Bologna (<https://cris.unibo.it/>).
When citing, please refer to the published version.

(Article begins on next page)

This is the final peer-reviewed accepted manuscript of:

L. Biancalana, E. Zanda, M. Hadiji, S. Zacchini, A. Pratesi, G. Pampaloni, P. J. Dyson, F. Marchetti, "Role of the (Pseudo)Halido Ligand in Ruthenium(II) p-Cymene α -Amino Acid Complexes on Speciation, Protein Reactivity and Cytotoxicity", *Dalton Trans.*, **2021**, 50, 15760-15777.

The final published version is available online at:

<https://doi.org/10.1039/d1dt03274g>

Terms of use:

Some rights reserved. The terms and conditions for the reuse of this version of the manuscript are specified in the publishing policy. For all terms of use and more information see the publisher's website.

Role of the (Pseudo)Halido Ligand in Ruthenium(II) *p*-Cymene α -Amino Acid Complexes on Speciation, Protein Reactivity and Cytotoxicity

Lorenzo Biancalana,^{a,} Emanuele Zanda,^{a,#} Mouna Hadiji,^b Stefano Zacchini,^c Alessandro Pratesi,^a
Guido Pampaloni,^a Paul J. Dyson^b and Fabio Marchetti^{a,*}*

*^aUniversity of Pisa, Dipartimento di Chimica e Chimica Industriale, Via G. Moruzzi 13, I-56124 Pisa,
Italy.*

*^b Institut des Sciences et Ingénierie Chimiques, Ecole Polytechnique Fédérale de Lausanne (EPFL),
Switzerland.*

*^cUniversity of Bologna, Dipartimento di Chimica Industriale “Toso Montanari”, Viale Risorgimento 4,
I-40136 Bologna, Italy.*

Corresponding Authors

*E-mail addresses: lorenzo.biancalana@unipi.it, fabio.marchetti1974@unipi.it

[#]Present address: Laboratoire de Physique des 2 Infinis Irène Joliot Curie (IJCLab), UMR 9012, CNRS/IN2P3 Université Paris-Saclay, 15 rue Georges Clemenceau, 91405 Orsay Cedex, France

Abstract

The reactions of the dimeric complexes $[\text{RuX}_2(\eta^6\text{-}p\text{-cymene})]_2$ ($\text{X} = \text{Br}, \text{I}, \text{SCN}$) with L-proline (ProH) and *trans*-4-hydroxy-L-proline (HypH), in methanol in the presence of NaOH, afforded $[\text{RuX}(\kappa^2\text{N},\text{O-Pro})(\eta^6\text{-}p\text{-cymene})]$ ($\text{X} = \text{Br}, \mathbf{1b}; \text{I}, \mathbf{1c}; \text{SCN}, \mathbf{1d}$) and $[\text{RuX}(\kappa^2\text{N},\text{O-Hyp})(\eta^6\text{-}p\text{-cymene})]$ ($\text{X} = \text{Br}, \mathbf{2b}; \text{I}, \mathbf{2c}; \text{SCN}, \mathbf{2d}$), respectively. Alternatively, the one-pot, sequential addition of the appropriate α -amino carboxylate and X^- salt to $[\text{RuCl}_2(\eta^6\text{-}p\text{-cymene})]_2$ led to $[\text{RuX}(\kappa^2\text{N},\text{O-Pro})(\eta^6\text{-}p\text{-cymene})]$ ($\text{X} = \text{N}_3, \mathbf{1e}; \text{NO}_2, \mathbf{1f}; \text{CN}, \mathbf{1g}$) and $[\text{Ru}(\text{N}_3)(\kappa^2\text{N},\text{O-Hyp})(\eta^6\text{-}p\text{-cymene})]$ ($\mathbf{2e}$). Complexes $[\text{Ru}(\kappa^3\text{N},\text{O},\text{O}'\text{-O}_2\text{CCH}(\text{NH}_2)(\text{R})\text{O})(\eta^6\text{-}p\text{-cymene})]$ ($\text{R} = \text{CH}_2, \mathbf{3h}; \text{R} = \text{CHMe}, \mathbf{4h}; \text{R} = \text{CH}_2\text{CH}_2, \mathbf{5h}$) were prepared from the reaction of $[\text{RuCl}_2(\eta^6\text{-}p\text{-cymene})]_2$ with the appropriate α -amino acid and NaOH in refluxing isopropanol. Treatment of $[\text{RuCl}(\kappa^2\text{N},\text{O-SerH})(\eta^6\text{-}p\text{-cymene})]$ ($\mathbf{3a}$) with PTA in water at reflux produced $[\text{Ru}(\kappa^2\text{N},\text{O-Ser})(\kappa\text{P-PTA})(\eta^6\text{-}p\text{-cymene})]\text{Cl}$ ($[\mathbf{3i}]\text{Cl}$). The products were isolated in good to excellent yields, and were characterized by elemental analysis, IR and multinuclear NMR spectroscopy. The structures of $\mathbf{1f}$ and $\mathbf{2b-e}$ were ascertained by X-ray diffraction studies. The behaviour of the complexes in water and cell culture medium was investigated by multinuclear NMR and UV-Vis spectroscopy, revealing a considerable influence of the monodentate ligand on the aqueous chemistry. The water-stable complexes $\mathbf{1d-e}, \mathbf{2d-e}, \mathbf{3h}, \mathbf{4h}$ and $[\mathbf{3i}]\text{Cl}$ were assessed for their cytotoxicity towards A2780 and A2780cisR cancer cell lines and the noncancerous HEK 293T cell line. A selection of compounds was also investigated for Ru uptake in A2780 cells and interactions with cytochrome c as a model protein. Combined, these studies provide insights into the previously debated role of the anionic monodentate 'leaving' ligand on the biological activity of Ru(II) arene α -amino acid complexes.

Keywords: Bioorganometallic Chemistry; Anticancer Metal Complexes; Metals in Medicine; Ruthenium(II) Arene Complexes; Halide Dissociation; Aquation

Introduction

The search for anticancer metal-based drugs as alternatives to platinum compounds continues to attract attention and different types of ruthenium complexes appear to show promise.¹ Beside the prototypal NAMI-A, KP1019 and related ruthenium(III) salts which underwent clinical trials,² ruthenium(II) arene complexes have attracted much attention; in particular, those containing a 1,3,5-triaza-7-phosphaadamantane (PTA) or bidentate ethylenediamine ligands, such as the representative compounds RAPTA-C and RM175 (Figure 1a-b).³ The activation of these pro-drugs is believed to initiate with chloride/water substitution (aquation), thus enabling subsequent metal binding to biological targets.⁴ It has been demonstrated also for a variety of other Ru^{II}-arene complexes that the release of the chloride ligand in physiological media is crucial, since it favours the interaction with biomolecules, and can result in inhibition of enzymes.³ The thermodynamics and kinetics of the aquation process of Ru(II)-arene complexes, and subsequent reactivity, is regulated by the arene substituents and the nature of other co-ligands.⁵ For instance, $[\text{RuCl}(\text{N}^{\wedge}\text{N})(\eta^6\text{-arene})]^+$ complexes containing a 1,2-diamine ($\text{N}^{\wedge}\text{N}$) ligand, including RM175, are labile towards Ru-Cl cleavage in aqueous solution, a process that is reversed on increasing the chloride concentration.⁶ Instead, complexes with unsaturated/aromatic $\text{N}^{\wedge}\text{N}$ ligands, such as α -diimines, pyridylimines or pyridylquinoxalines, are comparatively inert, the Ru-Cl bond being reinforced as a result of their π -acceptor character.⁷ However, arene loss was observed with strongly π -acceptor phenylazopyridine ligands.⁸ At the opposite extreme, complexes with monoanionic $\text{O}^{\wedge}\text{O}$ ligands such as carboxylates, hydroxy-pyr(id)ones and related species are often poorly stable in aqueous solution, also with respect to the bidentate ligand, leading to formation of a biologically inactive dimer, $[\text{Ru}_2(\mu\text{-OH})_3(\eta^6\text{-arene})_2]^+$, at physiological pH.⁹

In this setting, α -amino acid derivatives of general formula $[\text{RuCl}(\text{N}^{\wedge}\text{O})(\eta^6\text{-arene})]$ have gained interest in both catalysis and medicinal fields, as well as for their aggregation phenomena in solution,^{10,11,12,13} due to their straightforward synthesis and specific features of the amino-carboxylato

$\{N^{\wedge}O\}$ unit, *i.e.* widely available and nontoxic, structural variability given by different side-chains, enhanced water-solubility and chirality conferred to the resulting metal species. Despite early claims of *in vivo* anticancer activity,^{12a} most of these complexes are not cytotoxic against various cancer cell lines;^{12b,d,13} and are also ineffective as antimicrobials.^{12c}

Complexes $[RuCl(\alpha\text{-aminocarboxylato})(\eta^6\text{-arene})]$ undergo rapid and extensive aquation, which is considered to be responsible for the biological inactivity, with the resulting $[Ru(H_2O)(\alpha\text{-aminocarboxylato})(\eta^6\text{-arene})]^+$ species presumably sequestered by extracellular biomolecules.^{12b}

In this context, the replacement of the chloride with a different halide (Br^- , I^-) or pseudohalide (N_3^- , SCN^-) ligand offers the possibility of modifying the kinetics and thermodynamics of the aquation process in $[RuX(L^{\wedge}L)(\eta^6\text{-arene})]^{0/+}$ complexes ($L^{\wedge}L$ = generic bidentate ligand), and, potentially, their biological activity. In some cases, chlorido/iodide replacement or related structural modifications caused pronounced alterations to the cytotoxicity profile (potency, selectivity, cross-resistance), cellular accumulation and/or interaction with specific biomolecules, suggesting a major change in the mechanism of the anticancer action.¹⁴ Note that the iodide ion, once dissociated from the metal, might play a peculiar role in cell redox imbalance, acting as a catalyst for H_2O_2 decomposition in the mitochondria.^{14a}

In other cases, little or no difference in the biological activity was observed on varying the (pseudo)halido ligand.^{14b,g,15} Indeed, fast and extensive aquation in water^{15b-d,j} as well as (pseudo)halide/chloride exchange in the cell culture medium^{15a,f,g} result in the formation of the same ruthenium species, which presumably explains the similarities in the biological effects.

Herein, we report the synthesis and the characterization of a series of ruthenium(II) *p*-cymene α -aminocarboxylato complexes, with a variable anionic fragment completing the coordination set in the place of the chloride, comprising different halides, pseudo(halides) and alkoxy ligands belonging to the α -aminoacid side-chain. The relationship between such structural variability in the complexes and their

aqueous speciation, cytotoxicity, cellular uptake and interaction with a model protein is discussed. The results contribute to defining, to a more general extent, the role of aquation in the mechanism of action of anticancer ruthenium-arene species.

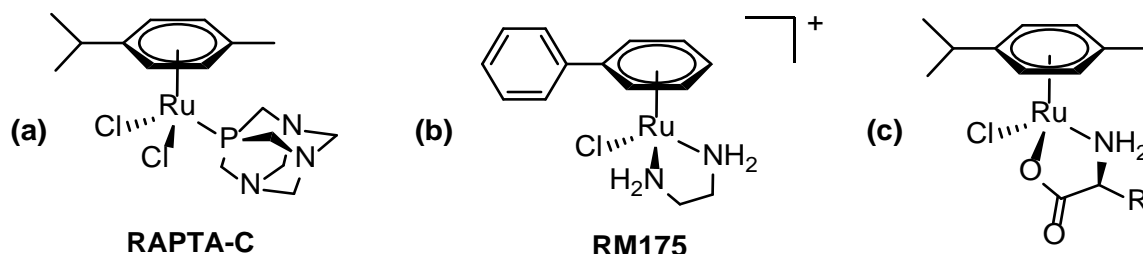


Figure 1. Ru^{II}(η^6 -arene) complexes with anticancer activity and chloride(s) leaving ligands: structures of RAPTA-C (a), RM175 (b) and α -amino carboxylate-*p*-cymene complexes (c).

Results and discussion

1. Synthesis

A series of ruthenium(II) α -amino-carboxylato complexes of general formula $[\text{RuX}(\alpha\text{-amino-carboxylate})(\eta^6\text{-}p\text{-cymene})]$ was prepared according to two synthetic strategies, consisting of chloride/(pseudo)halide exchange on the dimeric precursor $[\text{RuCl}_2(\eta^6\text{-}p\text{-cymene})]_2$ followed by addition of the α -amino carboxylate ligand, and the reverse sequence (Scheme 1, paths a and b). The first strategy was previously adopted to obtain azido derivatives $[\text{Ru}(\text{N}_3)(\alpha\text{-amino-carboxylate})(\eta^6\text{-}p\text{-cymene})]$ from $[\text{Ru}_2\text{Cl}_2(\mu\text{-N}_3)_2(\eta^6\text{-}p\text{-cymene})_2]$,¹⁶ whereas the latter afforded some $[\text{RuI}(\alpha\text{-amino-carboxylate})(\eta^6\text{-}p\text{-cymene})]$ complexes.¹⁷

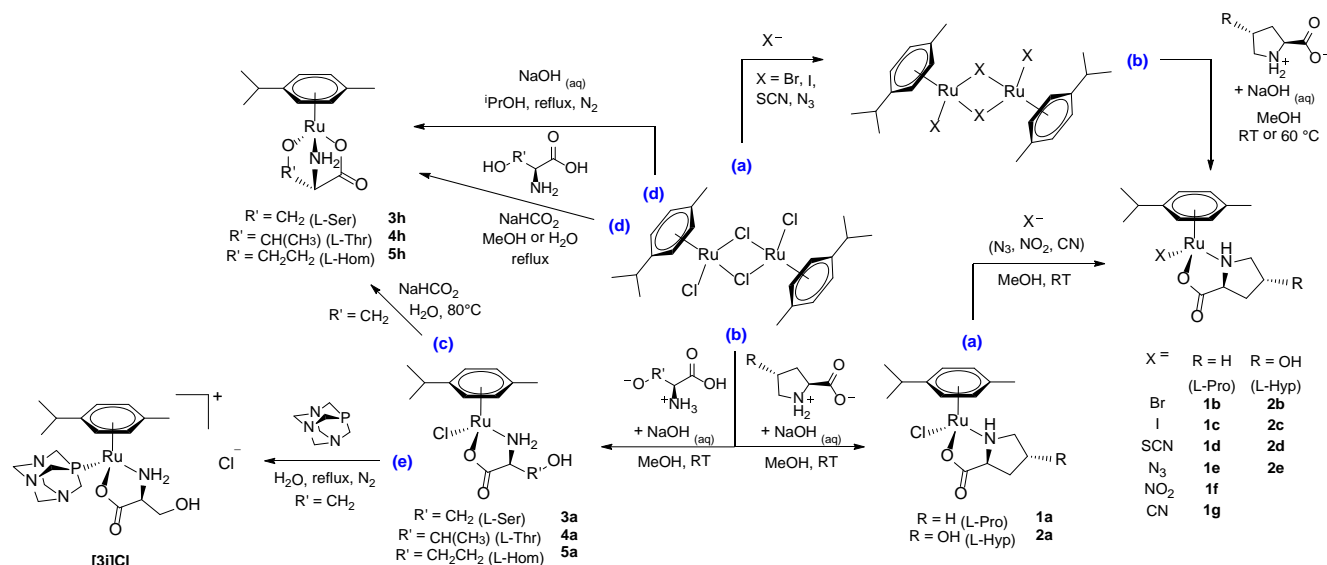
We obtained $[\text{RuX}_2(\eta^6\text{-}p\text{-cymene})]_2$ (X = Br, I, SCN) in quantitative yield from the reaction of $[\text{RuCl}_2(\eta^6\text{-}p\text{-cymene})]_2$ with an excess of the appropriate sodium/potassium salt, using a modification of the literature procedures.¹⁸ In this respect, acetone was found to be an optimal solvent for the reactions with NaI and KSCN, whereas an iterative reaction/extraction procedure was necessary in the case of NaBr. Next, treatment of $[\text{RuX}_2(\eta^6\text{-}p\text{-cymene})]_2$ (X = Br, I, SCN) with L-proline (ProH) or *trans*-4-

hydroxy-L-proline (HypH) in methanol in the presence of sodium hydroxide led to, respectively, **1b-d** and **2b-d**.

Attempts of chloride exchange on $[\text{RuCl}_2(\eta^6\text{-}p\text{-cymene})]_2$ with other anionic ligands did not proceed smoothly. Reactions with KCN and NaNO_2 in methanol were not selective and led to arene dissociation even under stoichiometric conditions, similarly to the reactivity of $[\text{RuCl}_2(\eta^6\text{-C}_6\text{H}_6)]_2$ with KCN in water.¹⁹ On the other hand, the reaction of $[\text{RuCl}_2(\eta^6\text{-}p\text{-cymene})]_2$ with NaN_3 , following the literature procedure for the synthesis of $[\text{Ru}(\text{N}_3)_2(\eta^6\text{-}p\text{-cymene})]_2$,²⁰ ended with an explosion during the work-up! Therefore, **1e-g** and **2e** were prepared from the one-pot reaction of $[\text{RuCl}_2(\eta^6\text{-}p\text{-cymene})]_2$ with the α -amino carboxylate, followed by the addition of the desired Na^+/K^+ (pseudo)halide. Compounds **1b-g** and **2b-e** were separated from the alkali metal salts by filtration with CH_2Cl_2 through celite and were isolated as yellow solids in 77-93 % yield.

A further approach to substitute the chloride ligand in $[\text{RuCl}(\alpha\text{-amino-carboxylate})(\eta^6\text{-}p\text{-cymene})]$ relies on the coordination of functional groups belonging to the α -amino acid side chain, exploiting the chelate effect.²¹ In this regard, we recently reported the selective formation of **3h**, featuring a dianionic tridentate L-serine, from **3a** and NaHCO_2 in water at 80 °C (Scheme 1 path c).¹³ Consequently, we attempted the direct, one-step synthesis of **3-5h** by reaction of $[\text{RuCl}_2(\eta^6\text{-}p\text{-cymene})]_2$ with alcohol-functionalized α -amino acids (L-serine, L-threonine and L-homoserine), in water in the presence of NaHCO_2 (Scheme 1 path d). However, the final products were contaminated with traces of **3-5a** and metal-hydride species. Notably, the rare bis-hydride $[\text{Ru}_2(\eta^6\text{-}p\text{-cymene})_2(\mu\text{-H})_2(\mu\text{-Cl})]^+$ was isolated once by silica chromatography ($\delta_{\text{H}} = -14$ ppm; Figure S50).²² Unfortunately, the outcome was not reproducible, in alignment with M. A. Bennett's comments on the elusive nature of the hexamethylbenzene analogue.^{22b} Switching to NaOH in isopropanol under reflux was pivotal in the selective and quantitative formation of **3-5h**, which were isolated as yellow solids, following MeCN extraction, in 79-85 % yield.

Complex **[3i]**Cl was prepared by reaction of **3a** with PTA in refluxing water under nitrogen and isolated in 95 % yield as an ochre-yellow solid (Scheme 1 path e). This successful example of chloride/phosphine exchange takes advantage of the lability of the Ru-Cl bond in aqueous medium and the water solubility of PTA, without needing to force chloride abstraction with silver salts.^{13,23}



Scheme 1. Preparation of ruthenium(II) arene complexes of α -aminoacids: **(a)**chloride/anionic ligand (X^-) exchange; **(b)** α -aminocarboxylate addition to $[RuX_2(\eta^6\text{-}p\text{-cymene})]_2$; **(c)**deprotonation and coordination of the alcoholic side-chain; **(d)**straightforward coordination of a tridentate dianionic alkoxy(α -amino)carboxylate ligand; **(e)**phosphine/chloride exchange. The path **(b)** then **(a)** was performed in one-pot, without isolation of **1-2a** (see Experimental for details). RT = room temperature.

2. Structural characterization

All non-chlorido complexes depicted in Scheme 1 are unprecedented, except **1c**, **1e** and **3h**,^{13,16,17} and include the first examples of ruthenium(II)-arene α -amino carboxylato complexes with Br^- , SCN^- , NO_2^- or CN^- co-ligands. The new compounds were fully characterized by analytical methods and IR and NMR spectroscopy (Figures S1-S56). NMR spectra of **1b-g**, **2b-e** and **[3i]Cl** (in CD_3OD) display two sets of resonances, due to the combined chirality at the metal centre and at the α -amino acid ligand (mixture of $S_{\text{C}}S_{\text{Ru}}$ and $S_{\text{C}}R_{\text{Ru}}$ diastereomers). Conversely, **3-5h** exist as a single enantiomer, due to stereochemical constraints of the tridentate coordination.^{13,21b} Isomer ratios in CD_3OD range from 1 (**2d**) to 6.5 (**1c**) and are generally higher for the prolinato species with respect to the hydroxyprolinato

counterparts (Table S1).²³In the case of L-serine derivatives, the isomer ratio is rather low (1.3-1.4) with chlorido (**3a**) and PTAcO-ligands (**[3i]⁺**), while the bulky PPh₃ ligand (reported elsewhere¹³) raises the value up to 5.

Spectroscopic fingerprints (IR, ¹³C and ¹⁴N NMR) of thiocyanate, azide, nitrite and cyanide ligands are collected in Table S2. Coordination of nitrite ligands to Ru(η^6 -arene) complexes occurs mostly via the nitrogen atom; conversely thiocyanate binding often results in linkage isomerism.²⁴In this regard, [Ru(SCN)₂(η^6 -*p*-cymene)]₂ exists as a mixture of isomers with various combinations of *N*- and *S*-bonded thiocyanate, based on IR (solid-state), ¹H and ¹³C NMR spectra (acetone-*d*₆),²⁵ as proposed for the homologous η^6 -benzene compound.¹⁹ Instead, thiocyanate and nitrite are *N*-coordinated in **1-2d** and **1f**, as indicated by solid-state IR²⁶ and X-ray structural data (vide infra).

The IR C-N stretching of **1g** is shifted by 28 cm⁻¹ to higher wavenumber with respect to KCN, indicating a certain degree of π -backbonding in the interaction.^{26,27,28} Also, the antisymmetric (1365 cm⁻¹) and symmetric (1304 cm⁻¹) stretching of the NO₂⁻ ligand in **1f** are at the edge of the typical wavenumber ranges, and the N-O interactions are weakened by π -backdonation.^{29,30} The IR spectrum of [Ru(N₃)₂(η^6 -*p*-cymene)]₂ contains two N-N stretching absorptions, due to bridging (2059 cm⁻¹) and terminal (2040 cm⁻¹) azido ligands, whereas the spectra of **1e-2e** display only one band at lower wavenumbers (ca. 2025 cm⁻¹). Coordination of NO₂⁻ and SCN⁻ ligands to {Ru(η^6 -*p*-cymene)} scaffolds led to a considerable shielding and broadening of the respective ¹⁴N NMR resonance, in comparison with the free ions (Na⁺/K⁺ salts); whereas a modest shielding effect was noticed for coordinated N₃⁻ (Figures S54-S56, Table S2).

The X-ray structures of **1f**, **2b**, **2c**, **2d** and **2e** were elucidated by single-crystal X-ray diffraction studies, and views of the structures are shown in Figures 2-3. In addition, the X-ray structure of the previously reported [Ru(N₃)₂(η^6 -*p*-cymene)]₂ (**Ru-N3**) is supplied as Supporting Information (Figure S57). Compounds **1f**, **2b**, **2c**, **2d** and **2e** display a three-leg piano-stool geometry, and bonding parameters (listed in the captions) are comparable to those previously reported for homologous

complexes. The Ru-C, Ru-N and Ru-O bond distances are not particularly affected by the different pseudo(halido)ligand (X) attached to the $\{\text{Ru}(\kappa^2\text{N},\text{O-L-Hyp})(\eta^6\text{-}p\text{-cymene})\}^+$ frame (X = Cl,¹⁷Br,I,SCN,N₃). All compounds crystallized as a single diastereomer, displaying the $S_C S_{Ru}$ configuration for **2b**, **c**, **e** and **1f** and $S_C R_{Ru}$ for **2c**.³¹ Enantiopurity in the crystal structures has been observed for related chloride counterparts, which rapidly epimerize in solution.^{13,17,32} As expected, an extensive network of hydrogen bonding between the amino, hydroxyl and carboxyl functions is present in the crystals of **2b-e** (Table S3).

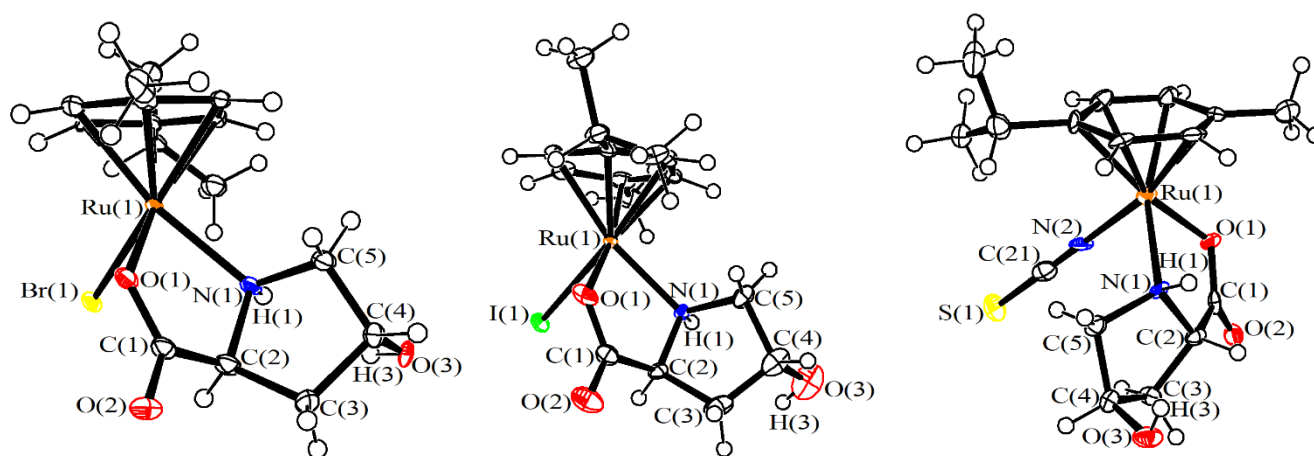


Figure 2. View of the structures of $[\text{RuBr}(\kappa^2\text{N},\text{O-Hyp})(\eta^6\text{-}p\text{-cymene})]$, **2b** (left), $[\text{RuI}(\kappa^2\text{N},\text{O-Hyp})(\eta^6\text{-}p\text{-cymene})]$, **2c** (middle) and $[\text{Ru}(\kappa\text{N-NCS})(\kappa^2\text{N},\text{O-Hyp})(\eta^6\text{-}p\text{-cymene})]$, **2d** (right). Displacement ellipsoids are at the 50% probability level. Main bond distances (Å) and angles (°) follow. **2b**: Ru(1)-(η⁶-p-cymene)_{average} 2.18(6), Ru(1)-O(1) 2.108(18), Ru(1)-N(1) 2.16(2), Ru(1)-Br(1) 2.525(3), O(1)-C(1) 1.29(3), C(1)-O(2) 1.24(3), C(1)-C(2) 1.53(4), C(2)-C(3) 1.51(4), C(3)-C(4) 1.60(4), C(4)-C(5) 1.51(4), N(1)-C(2) 1.55(3), N(1)-C(5) 1.49(4), C(4)-O(3) 1.46(2), Ru(1)-O(1)-C(1) 117.1(16), O(1)-C(1)-C(2) 119(2), C(1)-C(2)-N(1) 108(2), C(2)-N(1)-Ru(1) 109.6(17), O(1)-Ru(1)-N(1) 77.9(8). **2c**: Ru(1)-(η⁶-p-cymene)_{average} 2.19(4), Ru(1)-O(1) 2.144(11), Ru(1)-N(1) 2.142(12), Ru(1)-I(1) 2.7434(15), O(1)-C(1) 1.30(2), C(1)-O(2) 1.24(2), C(1)-C(2) 1.52(2), C(2)-C(3) 1.56(2), C(3)-C(4) 1.52(3), C(4)-C(5) 1.52(2), N(1)-C(2) 1.466(18), N(1)-C(5) 1.495(19), C(4)-O(3) 1.46(2), Ru(1)-O(1)-C(1) 114.2(9), O(1)-C(1)-C(2) 118.4(13), C(1)-C(2)-N(1) 109.4(12), C(2)-N(1)-Ru(1) 110.5(9), O(1)-Ru(1)-N(1) 76.2(4). **2d**: Ru(1)-(η⁶-p-cymene)_{average} 2.17(2), Ru(1)-O(1) 2.081(6), Ru(1)-N(1) 2.145(6), Ru(1)-N(2) 2.050(8), O(1)-C(1) 1.281(10), C(1)-O(2) 1.242(11), C(1)-C(2) 1.523(12), C(2)-C(3) 1.523(12), C(3)-C(4) 1.503(13), C(4)-C(5) 1.516(12), N(1)-C(2) 1.497(11), N(1)-C(5) 1.487(11), C(4)-O(3) 1.429(10), N(2)-C(21) 1.149(12), C(21)-S(1) 1.636(11), Ru(1)-O(1)-C(1) 115.8(5), O(1)-C(1)-C(2) 118.0(8), C(1)-C(2)-N(1) 111.9(7), C(2)-N(1)-Ru(1) 110.5(5), O(1)-Ru(1)-N(1) 79.8(2), Ru(1)-N(2)-C(21) 175.6(8), N(2)-C(21)-S(1) 179.0(9).

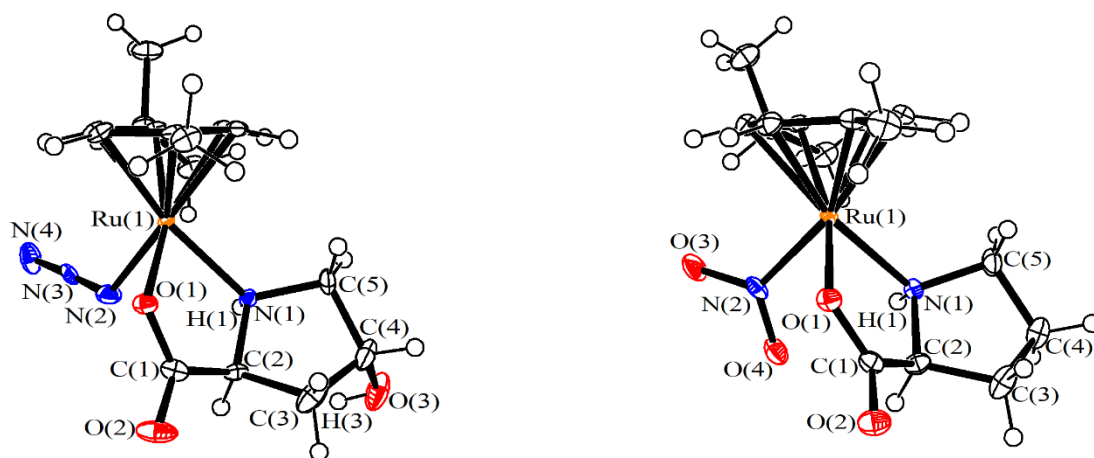


Figure 3. View of the structures of $[\text{Ru}(\text{N}_3)(\kappa^2\text{N},\text{O-Hyp})(\eta^6\text{-}p\text{-cymene})]$, **2e** (left) and $[\text{Ru}(\text{NO}_2)(\kappa^2\text{N},\text{O-Pro})(\eta^6\text{-}p\text{-cymene})]$, **1f** (right). Displacement ellipsoids are at the 50% probability level. Main bond distances (Å) and angles (°) follow. **2e**: $\text{Ru}(1)-(\eta^6\text{-}p\text{-cymene})_{\text{average}}$ 2.179(5), $\text{Ru}(1)-\text{O}(1)$ 2.0857(17), $\text{Ru}(1)-\text{N}(1)$ 2.124(2), $\text{Ru}(1)-\text{N}(2)$ 2.116(2), $\text{O}(1)-\text{C}(1)$ 1.286(3), $\text{C}(1)-\text{O}(2)$ 1.229(3), $\text{C}(1)-\text{C}(2)$ 1.519(3), $\text{C}(2)-\text{C}(3)$ 1.538(4), $\text{C}(3)-\text{C}(4)$ 1.517(5), $\text{C}(4)-\text{C}(5)$ 1.516(4), $\text{N}(1)-\text{C}(2)$ 1.501(3), $\text{N}(1)-\text{C}(5)$ 1.497(3), $\text{C}(4)-\text{O}(3)$ 1.431(3), $\text{N}(2)-\text{N}(3)$ 1.158(3), $\text{N}(3)-\text{N}(4)$ 1.183(3), $\text{Ru}(1)-\text{O}(1)-\text{C}(1)$ 116.86(15), $\text{O}(1)-\text{C}(1)-\text{C}(2)$ 117.2(2), $\text{C}(1)-\text{C}(2)-\text{N}(1)$ 112.49(19), $\text{C}(2)-\text{N}(1)-\text{Ru}(1)$ 110.51(15), $\text{O}(1)-\text{Ru}(1)-\text{N}(1)$ 79.54(7), $\text{Ru}(1)-\text{N}(2)-\text{N}(3)$ 121.76(19), $\text{N}(2)-\text{N}(3)-\text{N}(4)$ 176.5(3). **1f**: $\text{Ru}(1)-(\eta^6\text{-}p\text{-cymene})_{\text{average}}$ 2.203(5), $\text{Ru}(1)-\text{O}(1)$ 2.0694(17), $\text{Ru}(1)-\text{N}(1)$ 2.1262(18), $\text{Ru}(1)-\text{N}(2)$ 2.0888(18), $\text{O}(1)-\text{C}(1)$ 1.289(3), $\text{C}(1)-\text{O}(2)$ 1.236(3), $\text{C}(1)-\text{C}(2)$ 1.521(3), $\text{C}(2)-\text{C}(3)$ 1.536(3), $\text{C}(3)-\text{C}(4)$ 1.530(4), $\text{C}(4)-\text{C}(5)$ 1.522(3), $\text{N}(1)-\text{C}(2)$ 1.514(3), $\text{N}(1)-\text{C}(5)$ 1.501(3), $\text{N}(2)-\text{O}(3)$ 1.247(3), $\text{N}(2)-\text{O}(4)$ 1.242(3), $\text{Ru}(1)-\text{O}(1)-\text{C}(1)$ 118.71(15), $\text{O}(1)-\text{C}(1)-\text{C}(2)$ 117.5(2), $\text{C}(1)-\text{C}(2)-\text{N}(1)$ 111.52(18), $\text{C}(2)-\text{N}(1)-\text{Ru}(1)$ 111.08(14), $\text{O}(1)-\text{Ru}(1)-\text{N}(1)$ 79.70(7), $\text{O}(3)-\text{N}(2)-\text{O}(4)$ 118.5(2).

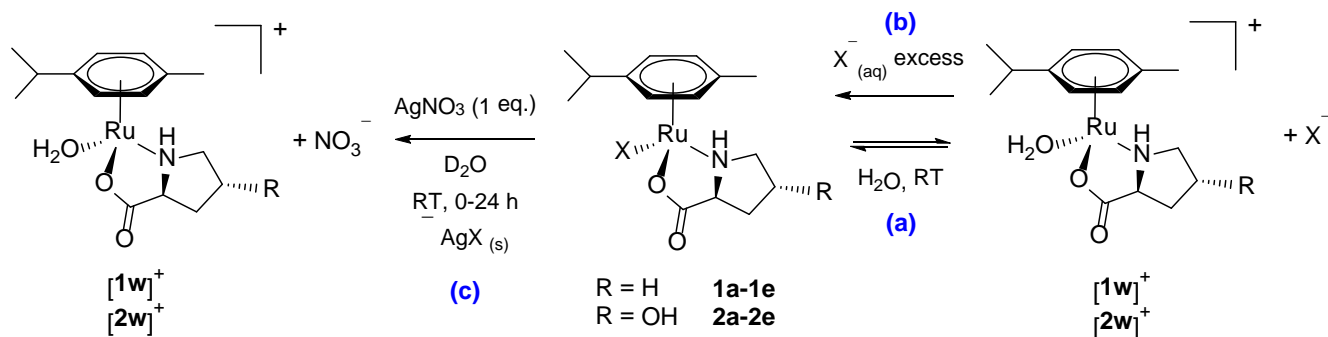
3. Speciation and stability in aqueous solution and cell culture medium

Aqueous solutions of **1a-e** and **2a-e** were analysed by NMR spectroscopy (D_2O , *ca.* 10^{-2} M), pH and conductivity measurements (H_2O , *ca.* 10^{-3} M), and the results are compiled in Table 1.

Compounds **1a-c** and **2a-c** undergo a rapid aquation of the ruthenium-halide bond, as indicated by the appearance of the diagnostic NMR resonance of $\text{Cl}^-_{(\text{aq})}$, $\text{Br}^-_{(\text{aq})}$ or $\text{I}^-_{(\text{aq})}$ ions, respectively (^{35}Cl , ^{81}Br and ^{127}I NMR).³³ The pH of the resulting solution (≈ 7) indicated the occurrence of a simple equilibrium between the starting halido and the cationic aquo complexes, $[\mathbf{1w}]^+ / [\mathbf{2w}]^+$ (Scheme 2a; four diastereomers).³⁴ Quantitative formation of halido or aquo complexes was observed upon addition of, respectively, an excess of sodium halide (Scheme 2b) or a stoichiometric amount of silver nitrate

(Scheme 2c), thus allowing unambiguous assignment of ^1H NMR signals (Figures S58-S60; S63-S65). According to NMR measurements, iodido complexes are more stable than their chlorido and bromido analogues, notwithstanding conductivity data indicate that the extent of aquation could be similar in more dilute solutions. Conductivity and pH measurements were almost unchanged after 24 h at room temperature, suggesting that equilibrium is rapidly attained. Conversely, thiocyanato (**1d-2d**) and azido (**1e-2e**) complexes are much less prone to aquation. Notably, the aquo species $[\mathbf{1w}]^+$ and $[\mathbf{2w}]^+$ were detected in the respective ^1H NMR spectra only after AgNO_3 addition (1 eq.), and this reaction was still incomplete after a few hours (Figures S61-S62; S66-S67). Conductivity data suggest limited aquation also in 10^{-3} M solutions, especially for the N_3^- complexes. According to ^1H NMR spectroscopy, D_2O solutions of **1d-2d** and **1e-2e** were practically unchanged after heating at 37°C for 48 hours (Table 1).

Scheme 2. Speciation in aqueous solution for $[\text{RuX}(\alpha\text{-aminocarboxylate})(p\text{-cymene})]$ complexes: equilibrium between aquo and (pseudo)halido complexes **(a)**; suppression of aquation by excess pseudo(halide) **(b)**; forced (pseudo)halide removal with AgNO_3 **(c)**. RT = room temperature.



Speciation of the complexes in a physiologically relevant medium was also investigated. Therefore, **1a-e** and **2a-e** were dissolved in deuterated DMEM cell culture medium (“DMEM-d”). Immediately after preparing the solutions, the two series of halido derivatives **1a-c** and **2a-c** displayed an almost identical ^1H NMR spectrum (Figures S68-S69),³⁵ indicating that the high chloride content of the medium (*ca.*

0.11 mol/L) leads the system to the same mixture of $\{\text{Ru}(\alpha\text{-aminocarboxylate})(p\text{-cymene})\}^+$ complexes. In contrast, ^1H NMR spectra of **1d-2d** ($X = \text{NCS}$) and **1e-2e** ($X = \text{N}_3$) in DMEM-d solution closely resemble those in D_2O , highlighting the substantial inertness towards X^- substitution (Figures S70-S73). Furthermore, thiocyanate and azide complexes appear sufficiently stable (66-75 %, Table 1) upon thermal treatment in the cell culture medium (37 °C, 24 h). Moreover, their (partial) transformation is not represented by the simple dissociation of $\text{SCN}^-/\text{N}_3^-$ ions, since peaks corresponding to aquo and chlorido complexes were not identified in the final ^1H NMR spectra. The tridentate derivatives **3h**, **4h** and the cationic **[3i]**⁺ are substantially more stable (Figures S74-S76 and Table 1), remaining almost intact in D_2O solution after 48 h at 37 °C and manifesting a marked stability also in DMEM-d solution at 37 °C.

Table 1. Stability of $[\text{RuX}(\alpha\text{-aminocarboxylate})(p\text{-cymene})]$ complexes in aqueous and cell culture media by ^1H NMR spectroscopy, pH and conductivity (see Experimental for details).

Compound	% Aquation [a,b]	pH [a]	$\Lambda_m^{[a,c]}$ ($\text{S}\cdot\text{cm}^2\cdot\text{mol}^{-1}$)	% Stability ^[d] (D_2O , 37 °C, 48 h)	% Stability ^[d] (DMEM-d, 37 °C, 24 h)
1a	65	7.1	100	–	–
1b	65	6.9	111	–	–
1c	30	6.9	103	–	–
1d	0	7.0	68	97 ^[e]	75 ^[e]
1e	0	7.2	31	99	66
2a	60	6.7	135	–	–
2b	55	6.7	109	–	–
2c	25	6.5	103	–	–
2d	0	6.5	69	98 ^[e]	67 ^[e]
2e	0	6.8	24	96	71
3h	0	7.0	15	99	88
4h	0	7.4	7	99	81
[3i]Cl	0	7.8	97	96	96

[a] Measured for the freshly-prepared solution at room temperature (≈ 21 °C) [b] Molar fraction of $[\text{Ru}(\text{D}_2\text{O})(\alpha\text{-aminocarboxylate})(p\text{-cymene})]^+$ (^1H NMR). [c] Reference conductivity data. $\Lambda_m(\text{H}_2\text{O}, 2.1\cdot 10^{-3} \text{ M})$: KCl, 146; KBr, 141; KI 141; KSCN 106; NaN_3 111 $\text{S}\cdot\text{cm}^2\cdot\text{mol}^{-1}$. [d] Residual amount of starting material with respect to the freshly-prepared solution (^1H NMR; Me_2SO_2 as internal standard). [e] $\text{D}_2\text{O}/\text{CD}_3\text{OD}$ or DMEM-d/ CD_3OD 5/2 v/v solutions.

4. Cytotoxicity

Bromido and iodo complexes **1b-c** and **2b-c** undergo rapid halide/chloride exchange in a biologically-relevant medium (*vide infra*) and were not investigated further, given the well-established non-cytotoxicity of $[\text{RuCl}(\kappa^2N,O\text{-}\alpha\text{-aminocarboxylate})(\eta^6\text{-arene})]$ complexes (see Introduction). Instead, **1d-e**, **2d-e**, **3h**, **4h** and **[3i]Cl** exhibited sufficient stability in the cell culture medium and were selected for cytotoxicity assays. The compounds were tested for antiproliferative activity on human ovarian carcinoma (A2780), its cisplatin resistant form (A2780cisR), and human embryonic kidney cell lines (HEK 293T), together with cisplatin and RAPTA-C as positive and negative controls, respectively. IC_{50} data after 72 h incubation are compiled in Table 2. All α -aminocarboxylate complexes revealed a limited cytotoxicity against the A2780 cell line, and were essentially inactive against A2780cisR and HEK 293T cells. For instance, the average IC_{50} of **1d,e**, **2d,e** and **3-4h** on the most sensitive cell line (A2780) is *ca.* 130-fold higher than cisplatin. The results are in alignment with those previously reported for the chloride analogues (see Introduction), indicating that changing the anionic ligand does not confer cytotoxicity to $\{\text{Ru}(\kappa^2N,O\text{-}\alpha\text{-aminocarboxylate})(\eta^6\text{-arene})\}$ complexes, and also suggesting that coordination of α -amino acids from the cell culture medium may represent a possible mechanism of deactivation for poorly cytotoxic and labile Ru(II) arene complexes in general.³⁶

Nevertheless, changing the anionic ligand has a marked influence on the reactivity of the investigated compounds in aqueous media, presumably influencing the biological activity. Additional experiments were performed to shed light on this point.

5. Water solubility, octanol-water partition coefficient and cellular uptake.

First, the solubility in water (D_2O) and octanol-water partition coefficients of the Ru complexes were assessed (Table 2). Most compounds are hydrophilic, featuring negative $\text{Log } P_{\text{ow}}$ values and/or high

water-solubility, reaching $0.2 \text{ mol}\cdot\text{L}^{-1}$ in some cases. In this respect, thiocyanato derivatives **1-2d** are less water-soluble and hydrophilic than their azido counterparts **1-2e**.

Table 2. Solubility in water (D_2O), octanol/water partition coefficients ($\text{Log}_{10} P_{\text{ow}}$) and cytotoxicity of ruthenium complexes on A2780, A2780cisR and HEK293T cell lines. IC_{50} values are given as the mean obtained from two independent experiments \pm standard deviation; cisplatin and RAPTA-C were used as control compounds.

Compound	Solubility / M (D_2O , 21°C)	Log P_{ow}	IC ₅₀ (72 h) / μM		
			A2780	A2780cisR	HEK293T
1d	$1.5\cdot 10^{-3}$	0.25 ± 0.08	69 ± 16	> 100	> 100
1e	$1.2\cdot 10^{-1}$	-0.26 ± 0.02	96 ± 3	> 100	> 100
2d	$1.8\cdot 10^{-2}$	-0.10 ± 0.05	71 ± 2	87 ± 4	> 100
2e	$5.0\cdot 10^{-2}$	< -1.5	73 ± 2	> 100	> 100
3h	$2.5\cdot 10^{-1}$	< -1.5	72 ± 3	> 100	> 100
4h	$2.1\cdot 10^{-1}$	< -1.5	87 ± 7	> 100	> 100
[3i]Cl	$> 2\cdot 10^{-2}$	$-1.5\text{-}1.8^{[c]}$	> 100	> 100	> 100
cisplatin ^[a]	$8.4\cdot 10^{-3}$	-2.19	0.6 ± 0.1	7.9 ± 0.1	2.6 ± 0.4
RAPTA-C ^[b]		$-1.5\text{-}1.8^{[c]}$	>200	>200	>200

[a] Literature values for solubility and Log P_{ow} . ³⁷[b] RAPTA-C = $[\text{RuCl}_2(\eta^6\text{-}p\text{-cymene})(\kappa P\text{-}1,3,5\text{-triaz-}7\text{-phosphaadamantane})]$. [c] Slightly below the limit of quantitation of the UV-vis technique ($-1.5 \leq \text{Log } P_{\text{ow}} \leq +1.5$).

Next, the internalization on A2780 cancer cells was investigated on a selection of compounds, namely L-proline derivatives with chlorido (**1a**) and thiocyanato (**1d**) co-ligands, complex **4h**, featuring a tridentate L-threonine residue, and the L-serine/PTA modified **[3i]⁺**. Ruthenium cellular content was measured by ICP-AES and the obtained results are summarised in Table 3. A poor cellular uptake was evidenced for all tested compounds that justifies their scarce cytotoxic effects. RAPTA-C, tested as a reference compound, is known to be poorly internalized and to exert its activity by interaction with extracellular components.^{3c} Presumably, cellular uptake is disfavoured due to the substantial hydrophilic character of substitutionally-inert compounds (**3h** and **[3i]Cl**), or their derivatives formed in the medium, due to rapid chloride replacement (**3a** and RAPTA-C³⁸). In this framework, the Ru uptake measured for **3d** is rather low, on considering the Log P_{ow} value (0.25; Table 2) and the stability in cell culture medium.

Table 3. Ruthenium content in A2780 cancer cells measured with ICP-AES.

Compound	Ru content (ng/10 ⁶ cells) ^[a]
1a	4.5 ± 1.4
1d	7.2 ± 2.9
4h	4.9 ± 1.5
[3i]Cl	7.0 ± 2.0
RAPTA-C	3.1 ± 1.6

[a] Mean of three different biological replicates. Control experiment: 1.2 ± 0.5 ng Ru/10⁶ cells.

6. Protein metalation

In order to gain a deeper insight into the reactivity in a biological environment, the interaction of the complexes with a small model protein, cytochrome c (Cyt c), was investigated. This protein has been widely investigated for its reactivity towards metal-based compounds using ESI-MS.³⁹ A three-fold molar excess of each complex (i.e. **1a**, **1d**, **4h**, and **[3i]Cl**) was incubated for up to 72 h with Cyt c in ammonium acetate solution at 37 °C, and the resulting mixtures were analysed by ESI-MS, according to a previously described protocol.⁴⁰ Figure 4 displays a representative ESI mass spectrum, depicting the Cyt c metalation status by **1a** after 24 h of incubation (the other spectra are shown in Figures S77-S83).

Adduct formation was observed with **1a**, **1d** and **4h**, whereas **[3i]**⁺ revealed a complete lack of reactivity with Cyt c (the signal at 12358 Da corresponds to the unreacted protein). A common adduct formed by **1a**, **1d** and **4h** corresponds to Cyt c with a {Ru(η^6 -*p*-cymene)} fragment (about 12591 Da), which implies the dissociation of the other ligands from the parent metal complex, as observed for several other ruthenium(II) arene compounds, including RAPTA-C.^{39c,41} The MS spectrum of **1a**/Cyt c also contains a peak at 12941 Da of low relative intensity corresponding to the protein derivatized with {Ru(*p*-cymene)} and {Ru(L-prolinato)(*p*-cymene)} fragments (Figure 4). Incubation with **1d** resulted

in a second adduct, formally corresponding to attachment of the $\{\text{Ru}(\text{SCN})(p\text{-cymene})\}$ unit⁴² to the protein (12651 Da; Figures S78-S79).

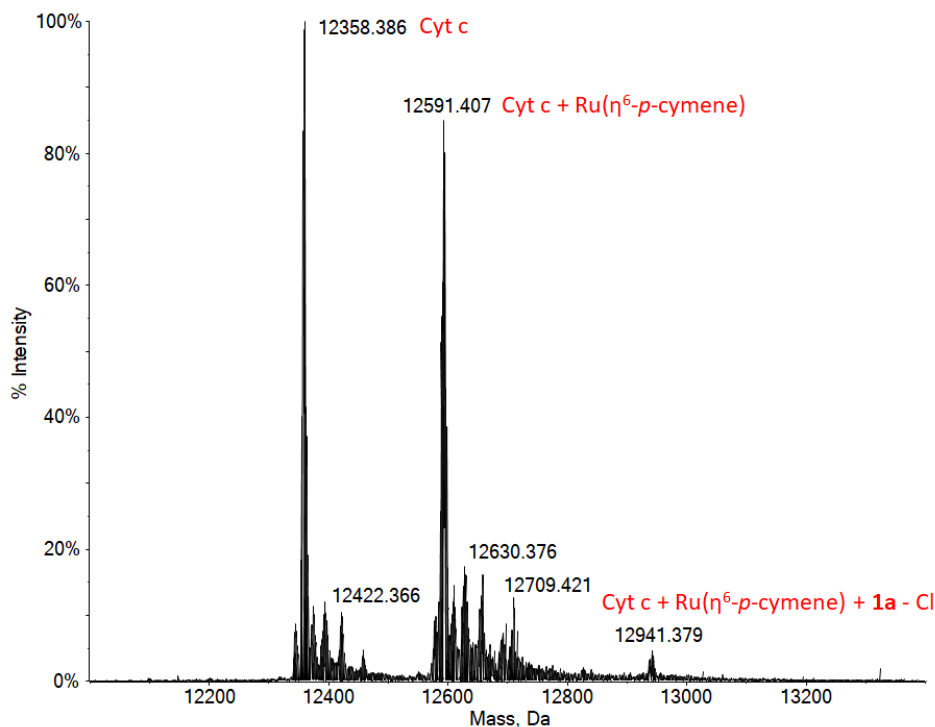


Figure 4. Deconvoluted ESI mass spectrum for 10^{-7} M cytochrome c in ammonium acetate solution (pH 6.8), incubated with **1a** for 24 h at 37 °C (metal to protein molar ratio = 3).

It is interesting to compare the reactivity of the selected compounds with respect to the fraction of ruthenated protein (Table 4). Incubation with **1a** for 24 h resulted in nearly 60 % of adducts formation. Under the same conditions, binding decreases along the series **1d** (44 %) > **4h** (16 %) > **[3i]⁺** (0 %). With the exception of **[3i]⁺**, protein metalation increases during the next 48 h, maintaining the same order of reactivity. The reactivity trend with Cyt c of the complexes is in alignment with previous stability studies in aqueous solution and in cell culture medium (Table 1). Notably, apart from the minor amount of the bis adduct with **1a**, the reaction with Cyt c implies the detachment of the α -aminocarboxylate ligand, that was not observed in protein-free medium. Therefore, the ease of dissociation of the anionic ligand (X) from $[\text{RuX}(\alpha\text{-aminocarboxylato})(p\text{-cymene})]$ complexes appears to regulate their binding to proteins, which may trigger further modifications, *i.e.* the release of the bidentate ligand. On the other

hand, the lack of an easily available coordination site prevents both aquation process(es) and reactivity with proteins.

Table 4. Cytochrome c metalation (% of protein metal adducts)^[a]

Compound	24 h	72 h
1a	61	90
1d	23	44
4h	5	16
[3i]Cl	0	0

[a]Calculated as the ratio between the sum of the areas corresponding to the smoothed MS peaks of the metal adducts and the total area of all the smoothed MS peaks in the mass spectrum.

Conclusions

We report the synthesis and a detailed crystallographic and spectroscopic characterization of a series of Ru(II) *p*-cymene α -amino acid complexes, the coordination sphere being completed by different anionic ligands such as(pseudo)halides, alkoxide group from the side-chain of hydroxy α -amino acids or the phosphane PTA. Such structural modifications have a considerable impact on the speciation of the complexes in water and in cell culture medium, their thermal stability and reactivity with a cytochrome c as a model protein. Despite these differences, all tested compounds show a limited cytotoxicity, which may be attributed to poor cellular uptake. Therefore, modifying the anionic ‘leaving’ ligand is not an effective strategy to confer cytotoxicity to the {Ru(α -aminocarboxylato)(arene)} scaffold. Basically, two different scenarios may be traced to explain why. Thus, bromide and iodide ligands are labile in saline solution and water replacement in [RuX(α -aminocarboxylato)(*p*-cymene)] complexes presumably initiates a deactivation process, ending with some protein binding via α -amino acid loss. On the other hand, the introduction of thiocyanate, azide or PTA as co-ligands, and the tridentate coordination of hydroxy α -amino acids, provides increased stability towards physiological components and proteins. The lack of activity of the most stable complexes is mainly due to their highly hydrophilic character.

Experimental

1. General experimental details

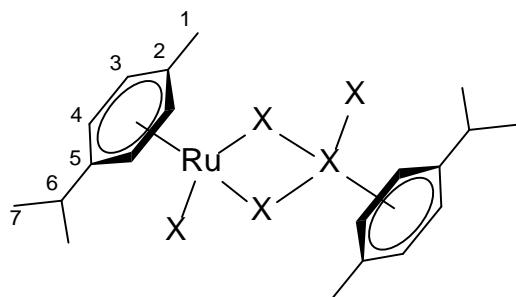
Ruthenium trichloride hydrate, L-proline (ProH), *trans*-4-hydroxy-L-proline (HypH), L-serine (SerH₂), L-threonine (ThrH₂), L-homoserine (HomH₂), 1,3,5-triaza-7-phosphaadamantane (PTA), other reactants and solvents were obtained from Alfa Aesar, Merck, Apollo Scientific or TCI Chemicals. NaOH 1.0 M in H₂O was prepared from Normex solution (Carlo Erba). [RuCl₂(η⁶-*p*-cymene)]₂,⁴³ [RuCl₂(η⁶-*p*-cymene)(κ*P*-1,3,5-triaza-7-phosphaadamantane)] (RAPTA-C)⁴⁴ and [RuCl(κ²*N,O*-L)(η⁶-*p*-cymene)]¹³ (L = Pro, **1a**; Hyp, **2a**; SerH, **3a**) were prepared as described in the literature; however an optimized preparation of **3a** is reported (see below). The preparation of **3-5h** and [**3i**]Cl was carried out under nitrogen with degassed solvents; all other synthetic operations were carried out in air with common laboratory glassware. Following their isolation in the solid-state, compounds were stored under dry N₂ as a general precaution due to the hygroscopic nature observed in some cases (*vide infra*); apart from this aspect, all compounds are air- and moisture-stable. NMR spectra were recorded at 25 °C on a Bruker Avance II DRX400 instrument equipped with a BBFO broadband probe. Chemical shifts (expressed in parts per million) are referenced to the residual solvent peaks (¹H, ¹³C) or to external standards (¹⁴N to CH₃NO₂, ³¹P to 85% H₃PO₄, ³⁵Cl, ⁸¹Br and ¹²⁷I to 0.1 M NaCl or 0.01 M NaBr or KI in D₂O, respectively). ⁴⁵ ¹H and ¹³C spectra were assigned with the assistance of ¹H-¹³C *gs*-HSQC experiments.⁴⁶ ¹H and ¹³C NMR resonances attributed to the minor isomer are italicized or, when possible, listed separately from those belonging to the major isomer. IR spectra of solid samples (650-4000 cm⁻¹) were recorded on a Perkin Elmer Spectrum One FT-IR spectrometer, equipped with a UATR sampling accessory. IR spectra were processed with Spectragryph software.⁴⁷ UV-Vis spectra were recorded on an Ultraspec 2100 Pro spectrophotometer, using 1 cm PMMA cuvettes. CHNS analyses were performed on a Vario MICRO cube instrument (Elementar). pH measurements were

performed with an Orion pH meter equipped with a Hamilton glass pH electrode, routinely calibrated with pH = 4.0 and 7.0 buffer solutions (Sigma-Aldrich). Conductivity measurements were carried out at 21 °C using an XS COND 8 instrument (cell constant = 1.0 cm⁻¹).⁴⁸

2. Synthesis and characterization of ruthenium complexes

[RuX₂(η⁶-*p*-cymene)]₂ (X = Br, I, NCS, N₃) (Chart 1).

Chart 1. Structure of [RuX₂(η⁶-*p*-cymene)]₂ (X = Br, I, NCS, N₃) (numbering refers to C atoms).



[RuBr₂(η⁶-*p*-cymene)]₂. A suspension of [RuCl₂(η⁶-*p*-cymene)]₂ (186 mg, 0.304 mmol) and NaBr (164 mg, 1.59 mmol) in a H₂O/MeOH 1:1 v/v mixture (*ca.* 10 mL) was vigorously stirred at room temperature for 2 h. Next, volatiles were removed under vacuum and the residue was suspended in CH₂Cl₂. The mixture was filtered through celite and the filtrate was dried under vacuum. NaBr (*ca.* 160 mg) was added, and the procedure was repeated (×3). The final residue was suspended in Et₂O and filtered. The resulting bright orange-red solid was washed with Et₂O and dried under vacuum (40 °C, over P₂O₅). Yield: 232 mg, 97%. Soluble in acetone, CH₂Cl₂, CHCl₃, poorly soluble in H₂O and E₂O. Anal. Calcd. For C₂₀H₂₈Br₄Ru₂: C, 30.40; H, 3.57. Found: C, 29.96; H, 3.38. IR (solid state): $\tilde{\nu}/\text{cm}^{-1}$ = 3048w, 3034m, 2956m, 2924m-sh, 2867w, 1527w, 1493m, 1469s, 1442s-sh, 1407m, 1385s, 1377s-sh, 1363m-sh, 1324m, 1274m, 1198m, 1156m, 1114m, 1087m, 1055s, 1028s-sh, 1004m, 957w, 825wm, 903w, 876s, 861s, 803s, 727s, 692m, 689m, 667m. ¹H NMR (CDCl₃): δ/ppm = 5.49 (d, ³J_{HH} = 5.9 Hz,

2H, C⁴H), 5.37 (d, ³J_{HH} = 5.9 Hz, 2H, C³H), 2.95 (h, ³J_{HH} = 6.9 Hz, 1H, C⁶H), 2.21 (s, 3H, C¹H), 1.26 (d, ³J_{HH} = 6.9 Hz, 6H, C⁷H).

[RuI₂(η⁶-*p*-cymene)]₂. A suspension of [RuCl₂(η⁶-*p*-cymene)]₂ (401 mg, 0.550 mmol) and NaI (597 mg, 3.98 mmol) in acetone (35 mL) was stirred at reflux temperature for 2.5 h. The resulting red/violet suspension was cooled to room temperature and taken to dryness under vacuum. The residue was suspended in CH₂Cl₂ and the suspension was filtered twice on a celite pad. Volatiles were removed under vacuum from the filtrate solution, affording a dark Bordeaux-red solid. The solid was washed with hexane then dried under vacuum (40 °C, over P₂O₅). Yield: 577 mg, 90%. Soluble in acetone, CH₂Cl₂, CHCl₃, poorly soluble in EtOH, Et₂O, insoluble in H₂O, petroleum ether and MeOH. Anal. Calcd. For C₂₀H₂₈I₄Ru₂: C, 24.56; H, 2.89. Found: C, 24.79; H, 2.77. IR (solid state): $\tilde{\nu}/\text{cm}^{-1}$ = 3028w, 2961m, 2924w, 2866w, 1902w, 1865w, 1785w, 1759w, 1735w, 1689w, 1530w, 1496w, 1469s, 1441w, 1407w, 1381s, 1375s, 1359m-sh, 1324w, 1296m, 1277m, 1211m, 1197m, 1156m, 1141m, 1115m, 1085m, 1055s, 1025s, 1006m, 958w, 923m, 888m, 866s, 801m, 734w, 659w. ¹H NMR (CDCl₃): δ/ppm = 5.53 (d, ³J_{HH} = 5.9 Hz, 2H, C⁴H), 5.43 (d, ³J_{HH} = 5.8 Hz, 2H, C³H), 3.01 (hept, ³J_{HH} = 6.9 Hz, 1H, C⁶H), 2.36 (s, 3H, C¹H), 1.25 (d, ³J_{HH} = 6.9 Hz, 6H, C⁷H).

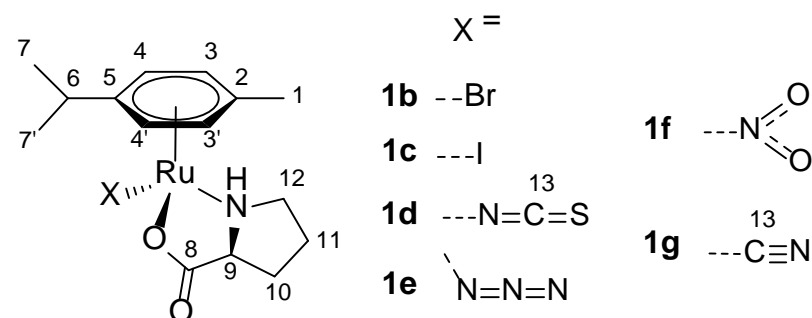
[Ru(SCN)₂(η⁶-*p*-cymene)]₂. Prepared as described for [RuI₂(η⁶-*p*-cymene)]₂, using [RuCl₂(η⁶-*p*-cymene)]₂ (111 mg, 0.181 mmol), KSCN (85 mg, 0.87 mmol) and acetone (10 mL). Orange solid; yield: 126 mg, 99%. Soluble in acetone, CH₂Cl₂, CHCl₃, MeOH, acetone, insoluble in E₂O. Anal. Calcd. For C₁₂H₁₄N₂RuS₂: C, 41.01; H, 4.02; N, 7.97; S, 18.24. Found: C, 41.0; H, 3.88; N, 7.35; S, 18.2. IR (solid state): $\tilde{\nu}/\text{cm}^{-1}$ = 3056w, 2963w, 2924w, 2870w; 2146s-sh, 2094s (νSCN); 1696w, 1534w, 1502w, 1468m, 1442w, 1388w, 1377w, 1363w, 1324w, 1279w, 1199w, 1159w, 1112w, 1089w, 1056w, 1030w, 1005w, 913w, 873m, 819w, 804w, 770w, 727w, 672w. ¹H NMR (CDCl₃): δ/ppm = 5.9–5.2 (br, 4H, C³H + C⁴H), 3.0–2.7 (br, 1H, C¹H), 2.4–2.2 (br, 3H, C⁶H), 1.5–1.3 (br, 6H, C⁷H). ¹H NMR (acetone-d₆): δ/ppm = 5.67, 5.59, 5.52, 5.42, 5.40, 5.33, 5.21 (d, ³J_{HH} = 6 Hz, 4H, C³H + C⁴H); 2.88–2.79 (m, 1H, C⁶H); 2.28, 2.24, 2.20 (s, 3H, C¹H); 1.39–1.30 (m, 6H, C⁷H).

$^{13}\text{C}\{^1\text{H}\}$ NMR (acetone- d_6): δ/ppm = 136.5, 136.0, 133.8 ($\kappa\text{N-SCN}$); 125.2 ($\kappa\text{S-SCN}$); 105.5, 104.7 (C^5); 100.9, 99.8 (C^2); 86.7, 86.5, 86.2, 84.4, 81.9 ($\text{C}^3 + \text{C}^4$); 31.8, 31.6, 31.4 (C^6); 22.4 (C^7); 19.0, 18.7, 18.3 (C^1). ^{14}N NMR (acetone/ C_6D_6): δ/ppm = - 279 ($\Delta\nu_{1/2}$ = 290 Hz, SCN).

$[\text{Ru}(\text{N}_3)_2(\eta^6\text{-}p\text{-cymene})]_2$. *WARNING: the solid product exploded during the reaction work-up!* A suspension of $[\text{RuCl}_2(\eta^6\text{-}p\text{-cymene})]_2$ (101 mg, 0.165 mmol) and NaN_3 (65 mg, 1.0 mmol) in EtOH (10 mL) was stirred at reflux temperature for 4 h. The resulting bright orange mixture was cooled to room temperature and volatiles were removed under vacuum. The residue was suspended in CH_2Cl_2 , and the suspension was filtered on a celite pad. Volatiles were removed under vacuum, affording an orange solid. *WARNING!* An explosion occurred while using a spatula to collect the solid from a G3 sintered-glass filter, leaving a black residue. X-ray quality crystals of $[\text{Ru}(\text{N}_3)_2(\eta^6\text{-}p\text{-cymene})]_2$ were obtained from a CH_2Cl_2 solution layered with hexane and settled aside at -20 °C. IR (solid state): $\tilde{\nu} / \text{cm}^{-1}$ = 3296w, 3052w, 2962w, 2928w, 2875w; 2059vs, 2040vs (νN_3), 1713w, 1465w, 1390w, 1380w, 1362w, 1340w, 1325w, 1284w, 1260m, 1220w, 1201w, 1162w, 1144w, 1088w, 1057w, 1031w, 1005w, 968w, 869m, 803w. ^1H NMR (CDCl_3): δ/ppm = 5.35 (d, $^3J_{\text{HH}}$ = 5.7 Hz, 2H, C^4H), 5.29 (d, $^3J_{\text{HH}}$ = 5.7 Hz, 2H, C^3H), 2.85 (hept, $^3J_{\text{HH}}$ = 6.8 Hz, 1H, C^6H), 2.24 (s, 1H, C^1H), 1.31 (d, $^3J_{\text{HH}}$ = 6.9 Hz, 6H, C^7H). ^{14}N NMR (acetone/ C_6D_6): δ/ppm = - 129, - 234 ($\Delta\nu_{1/2} \approx 130$ Hz, N_3).

$[\text{RuX}(\kappa^2\text{N},\text{O-Pro})(\eta^6\text{-}p\text{-cymene})]$, 1b-g (Chart 2).

Chart 2. Structures of 1a-g (numbering refers to C atoms).



General procedure A. A suspension of $[\text{RuX}_2(\eta^6\text{-}p\text{-cymene})]_2$ ($\text{X} = \text{Br, I, SCN}$; 20–60 mg) and L-proline (ProH, 2 eq) in MeOH (5 mL) was treated with NaOH (1.0 M solution in water; 2 eq). The mixture was stirred at room temperature for 4 h ($\text{X} = \text{I}$) or heated at 60 °C for 3 h ($\text{X} = \text{Br, SCN}$). Next, volatiles were removed under vacuum and the residue was suspended in CH_2Cl_2 . The suspension was filtered on a celite pad and the filtrate was dried under vacuum. The resulting solid was washed with Et_2O and dried under vacuum (40 °C).

General procedure B. A suspension of $[\text{RuCl}_2(\eta^6\text{-}p\text{-cymene})]_2$ (ca. 40 mg) and L-proline (ProH, 2 eq) in MeOH (5 mL) was treated with NaOH (1.0 M solution in water; 2 eq) and stirred at room temperature for 2 h, affording a yellow solution. Next, NaN_3 , NaNO_2 or KCN (2.2–2.6 eq) was added and the mixture was stirred at room temperature. After 5 hours, volatiles were removed under vacuum and the residue was treated as described above.

$[\text{RuBr}(\kappa^2\text{N},\text{O-Pro})(\eta^6\text{-}p\text{-cymene})]$, 1b. Prepared from $[\text{RuBr}_2(\eta^6\text{-}p\text{-cymene})]_2$ (52 mg, 0.066 mmol) and ProH (16 mg, 0.14 mmol) according to general procedure A. Slightly hygroscopic yellow-orange solid. Yield: 48 mg, 85%. Soluble in MeOH, CH_2Cl_2 , H_2O and THF, insoluble in Et_2O . Anal. Calcd. For $\text{C}_{15}\text{H}_{22}\text{BrNO}_2\text{Ru}$: C, 41.96; H, 5.16; N, 3.26. Found: C, 42.08; H, 5.04; N, 3.32. IR (solid state): $\tilde{\nu}/\text{cm}^{-1} = 3409\text{w-br}$ (νNH), 3160w-br, 3059w-br, 2961m, 2927m-sh, 2872m, 1610s-br, ($\nu_{\text{asym}}\text{CO}_2$), 1562m-sh, 1498w, 1468m-sh, 1446m, 1386m-sh ($\nu_{\text{sym}}\text{CO}_2$), 1362s-br, 1316m, 1299m, 1262m, 1199w, 1111w, 1088w, 1073w, 1055w, 1033w, 988w, 930w, 867w, 803w. ^1H NMR (CD_3OD , major isomer): $\delta/\text{ppm} = 5.68, 5.62$ (d, $^3J_{\text{HH}} = 6.0$ Hz, 2H, $\text{C}^4\text{H} + \text{C}^{4'}\text{H}$); 5.52, 5.47 (d, $^3J_{\text{HH}} = 5.8$ Hz, 2H, $\text{C}^3\text{H} + \text{C}^3'\text{H}$); 3.95 (dd, $^2J_{\text{HH}} = 11.0$ Hz, $^3J_{\text{HH}} = 5.8$ Hz, 1H, C^{12}H), 3.52 (dd, $^3J_{\text{HH}} = 9.4, 7.3$ Hz, 2H, C^9H), 3.10 (td, $^2J_{\text{HH}} = 11.3$ Hz, $^3J_{\text{HH}} = 6.1$ Hz, 1H, $\text{C}^{12}\text{H}'$), 2.87 (hept, $^3J_{\text{HH}} = 6.9$ Hz, 1H, C^6H), 2.19 (s, 3H, C^1H), 2.16–2.09 (m, 1H, C^{10}H), 1.97–1.88 (m, 1H, C^{11}H), 1.79–1.66 (m, 2H, $\text{C}^{10}\text{H}'$, $\text{C}^{11}\text{H}'$); 1.35, 1.29 (d, $^3J_{\text{HH}} = 6.9$ Hz, 6H, $\text{C}^7\text{H} + \text{C}^{7'}\text{H}$). ^1H NMR (CD_3OD , minor isomer): $\delta/\text{ppm} = 5.84, 5.77, 5.40$ (d, $J = 5.7$ Hz, 3H, $\text{C}^3\text{H} + \text{C}^4\text{H}$), 2.16 (s, 3H, C^1H). Isomer ratio ≈ 8 (^1H NMR, CD_3OD). $^{13}\text{C}\{^1\text{H}\}$ NMR (CD_3OD):

$\delta/\text{ppm} = 186.4$ (C^8), 102.3 (C^5), 96.8 (C^2); 85.1 , 84.5 ($\text{C}^3 + \text{C}^4$); 80.9 , 80.4 ($\text{C}^{3'} + \text{C}^{4'}$); 64.0 (C^9), 58.7 (C^{12}), 32.3 (C^6), 30.0 (C^{10}), 27.9 (C^{11}); 23.0 , 22.3 ($\text{C}^7 + \text{C}^{7'}$); 18.5 (C^1).

[RuI($\kappa^2\text{N},\text{O-Pro}$)($\eta^6\text{-p-cymene}$)], **1c.** Compound previously obtained from **1a** / NaI.¹⁷ Prepared from $[\text{RuI}_2(\eta^6\text{-p-cymene})]_2$ (50 mg, 0.051 mmol) and ProH (12 mg, 0.10 mmol) according to general procedure A. Orange solid. Yield: 38 mg, 78%. Soluble in MeOH, CH_2Cl_2 , H_2O and THF, insoluble in Et_2O . Anal. Calcd. For $\text{C}_{15}\text{H}_{22}\text{INO}_2\text{Ru}$: C, 37.82; H, 4.66; N, 2.94. Found: C, 37.66; H, 4.73; N, 2.88. IR (solid state): $\tilde{\nu}/\text{cm}^{-1} = 3421\text{w-br}$ (νNH), $3112\text{--}3056\text{w-br}$, 2961m , 2928m , 2869m , 1614s-br , ($\nu_{\text{asym}}\text{CO}_2$), 1563s-sh , 1497w , 1469m , 1445m , 1386m-sh ($\nu_{\text{sym}}\text{CO}_2$), 1362s-br , 1316m , 1299m , 1265w , 1199w , 1157w , 1113w , 1089w , 1055m , 1035m , 985w , 927m , 865m , 803m , 730w , 693w , 668w . ^1H NMR (CD_3OD , major isomer): $\delta/\text{ppm} = 5.80$ (d, $^3J_{\text{HH}} = 5.9$ Hz, 1H, C^4H), $5.68\text{--}5.64$ (m, 2H, $\text{C}^{4'}\text{H}$, $\text{C}^{3'}\text{H}$), 5.49 (d, $^3J_{\text{HH}} = 6.0$ Hz, 1H, C^3H), 3.97 (dd, $^2J_{\text{HH}} = 11.0$, $^3J_{\text{HH}} = 5.9$ Hz, 1H, C^{12}H), 3.58 (dd, $^3J_{\text{HH}} = 9.5$, 7.0 Hz, 1H, C^9H), 3.12 (td, $^2J_{\text{HH}} = 11.2$, $^3J_{\text{HH}} = 5.9$ Hz, 1H, $\text{C}^{12}\text{H}'$), 2.89 (hept, $^3J_{\text{HH}} = 6.9$ Hz, 1H, C^6H), 2.20 (s, 3H, C^1H), $2.15\text{--}2.09$ (m, 1H, C^{10}H), $1.99\text{--}1.89$ (m, 1H, C^{11}H), $1.81\text{--}1.70$ (m, 2H, $\text{C}^{10}\text{H}' + \text{C}^{11}\text{H}'$); 1.34 , 1.29 (d, $^3J_{\text{HH}} = 6.9$ Hz, 6H, $\text{C}^7\text{H} + \text{C}^{7'}\text{H}$). ^1H NMR (CD_3OD , minor isomer): $\delta/\text{ppm} = 5.89$, 5.78 , 5.74 , 5.57 ($^3J_{\text{HH}}$, $J = 5.8$ Hz, 4H, $\text{C}^3 + \text{C}^{3'} + \text{C}^4 + \text{C}^{4'}$); $3.71\text{--}3.64$ (m, 2H, $\text{C}^9 + \text{C}^{12}$), 2.17 (s, 3H, C^1), $2.10\text{--}2.01$ (m, 1H, C^{10}), 1.30 (d, $^3J_{\text{HH}} = 6.4$ Hz, 6H, $\text{C}^7 + \text{C}^{7'}$). Isomer ratio = 6.5 (^1H NMR, CD_3OD). $^{13}\text{C}\{^1\text{H}\}$ NMR (CD_3OD): $\delta/\text{ppm} = 186.3$ (C^8), 102.5 (C^5), 97.2 (C^2); 85.4 85.2 ($\text{C}^3 + \text{C}^4$); 81.0 , 80.6 ($\text{C}^{3'} + \text{C}^{4'}$); 65.2 (C^9), 59.3 (C^{12}), 32.6 (C^6), 29.8 (C^{10}), 28.0 (C^{11}); 23.4 , 22.3 ($\text{C}^7 + \text{C}^{7'}$); 18.9 (C^1).

[Ru($\kappa\text{N-NCS}$)($\kappa^2\text{N},\text{O-Pro}$)($\eta^6\text{-p-cymene}$)], **1d.** Prepared from $[\text{Ru}(\text{SCN})_2(\eta^6\text{-p-cymene})_2]_2$ (19 mg, 0.027 mmol) and ProH (12 mg, 0.10 mmol) according to general procedure A. Ochre yellow-orange solid. Yield: 20 mg, 91%. Soluble in EtOH, CH_2Cl_2 , DMSO, THF, scarcely soluble in MeOH, water and insoluble in Et_2O . Anal. Calcd. For $\text{C}_{16}\text{H}_{22}\text{N}_2\text{O}_2\text{RuS}$: C, 47.16; H, 5.44; N, 6.87; S, 7.87. Found: C, 47.05; H, 5.56; N, 6.93; S, 7.85. IR (solid state): $\tilde{\nu}/\text{cm}^{-1} = 3408\text{w-br}$ (νNH), 3215w-br , 3055w-br , 2967w , 2925w , 2873w ; 2094s-br , 2054m-sh (νSCN); 1615s-br ($\nu_{\text{asym}}\text{CO}_2$), 1494w , 1468w , 1447w ,

1386m-sh ($\nu_{\text{sym}}\text{CO}_2$), 1366s-br, 1317m, 1302m, 1263w, 1199w, 1159w, 1113w, 1079m, 1055m, 1035m, 983w, 931w, 868m, 842w, 823m, 804m, 792w, 671w. ^1H NMR (CD_3OD , major isomer): δ/ppm = 5.89 (m-br, 1H, NH); 5.81, 5.67 (d, $^3J_{\text{HH}} = 5.9$ Hz, 2H, $\text{C}^3\text{H} + \text{C}^4\text{H}$); 5.64, 5.47 (d, $^3J_{\text{HH}} = 5.9$ Hz, 2H, $\text{C}^{3'}\text{H} + \text{C}^{4'}\text{H}$); 3.99–3.89 (m, 1H, C^{12}H); *ca.* 3.30 (C^9H ; hidden by CD_2H); 3.04–2.90 (m, 1H, $\text{C}^{12}\text{H}'$), 2.87–2.75 (m, C^6H), 2.17 (s, 3H, C^1H), 2.22–2.08 (m, 1H, C^{10}H), 1.97–1.89 (m, 1H, C^{11}H), 1.86–1.67 (m, 2H, $\text{C}^{10}\text{H}' + \text{C}^{11}\text{H}'$); 1.35, 1.32 (d, $^3J_{\text{HH}} = 6.9$ Hz, 6H, $\text{C}^7\text{H} + \text{C}^{7'}\text{H}$). ^1H NMR (CD_3OD , minor isomer): δ/ppm = 7.62 (m-br, 1H, NH); 5.75, 5.72 (d, $^3J_{\text{HH}} = 5.9$ Hz, 2H, $\text{C}^3\text{H} + \text{C}^4\text{H}$); 5.61, 5.53 (d, $^3J_{\text{HH}} = 5.9$ Hz, 2H, $\text{C}^{3'}\text{H} + \text{C}^{4'}\text{H}$), 3.63 (q, $J = 8.5$ Hz, 1H, C^{12}H), 2.16 (s, 3H, C^1H), 1.36–1.29 (m, $\text{C}^7\text{H} + \text{C}^{7'}\text{H}$). Isomer ratio = 2 (^1H NMR, CD_3OD). $^{13}\text{C}\{^1\text{H}\}$ NMR (CD_3OD): δ/ppm = 185.7 (C^8), 138.7 (C^{13}), 103.5 (C^5), 98.8 (C^2); 85.3, 84.1 ($\text{C}^3 + \text{C}^4$); 82.2, 81.9 ($\text{C}^{3'} + \text{C}^{4'}$); 63.3 (C^9), 58.3 (C^{12}), 32.4 (C^6), 30.0 (C^{10}), 27.7 (C^{11}); 22.8, 22.6 ($\text{C}^7 + \text{C}^{7'}$); 18.3 (C^1). ^{14}N NMR (acetone/ C_6D_6): δ/ppm = – 258sh., – 264 ($\Delta\nu_{1/2} = 3 \cdot 10^2$ Hz, SCN).

[Ru(N₃)($\kappa^2\text{N},\text{O-Pro}$)($\eta^6\text{-}p\text{-cymene}$)], 1e. Compound previously obtained from $[\text{Ru}_2\text{Cl}_2(\mu\text{-N}_3)_2(\eta^6\text{-}p\text{-cymene})_2]$ and ProH. ¹⁶Prepared from $[\text{RuCl}_2(\eta^6\text{-}p\text{-cymene})]_2$ (42 mg, 0.069 mmol), ProH (16 mg, 0.14 mmol) and NaN_3 (12 mg, 0.18 mmol) according to general procedure **B**. Yellow-orange hygroscopic solid, stored under dry N_2 . Yield: 50 mg, 93%. Soluble in water, MeOH, CH_2Cl_2 , insoluble in Et_2O . Anal. Calcd. For $\text{C}_{15}\text{H}_{22}\text{N}_4\text{O}_2\text{Ru}$: C, 46.02; H, 5.66; N, 14.31. Found: C, 45.95; H, 5.73; N, 17.28. IR (solid state): $\tilde{\nu}/\text{cm}^{-1}$ = 3440w-br (νNH), 3160w-br, 3060w-sh, 2962m, 2926w-sh, 2871w, 2027s-br (νN_3), 1610s-br ($\nu_{\text{asym}}\text{CO}_2$), 1497w, 1469m, 1447m, 1361m-br ($\nu_{\text{sym}}\text{CO}_2$), 1316m, 1298m, 1285m, 1199w, 1157w, 1114w, 1089w, 1077w, 1055m, 1035m, 1003w, 983w, 931m, 868m, 803m, 768w, 729w, 695w, 670w. ^1H NMR (CD_3OD , major isomer): δ/ppm = 5.69, 5.56 (d, $^3J_{\text{HH}} = 5.9$ Hz, 2H, $\text{C}^3\text{H} + \text{C}^4\text{H}$); 5.52, 5.40 (d, $^3J_{\text{HH}} = 5.9$ Hz, 2H, $\text{C}^{3'}\text{H} + \text{C}^{4'}\text{H}$), 3.87 (dd, $^2J_{\text{HH}} = 11.0$ Hz, $^3J_{\text{HH}} = 5.9$ Hz, 1H, C^{12}H), 3.27 (dd, $^3J_{\text{HH}} = 9.1, 7.2$ Hz, 1H, C^9H), 3.09–3.00 (m, 1H, $\text{C}^{12}\text{H}'$), 2.89–2.79 (m, 1H, C^6H), 2.20 (s, 3H, C^1H), 2.16–2.05 (m, 1H, C^{10}H), 1.95–1.82 (m, 1H, C^{11}H), 1.80–1.65 (m, 2H, $\text{C}^{10}\text{H}' + \text{C}^{11}\text{H}'$); 1.36, 1.31 (d, $^3J_{\text{HH}} = 6.9$ Hz, 6H, $\text{C}^7\text{H} + \text{C}^{7'}\text{H}$). ^1H NMR (CD_3OD , minor isomer): δ/ppm =

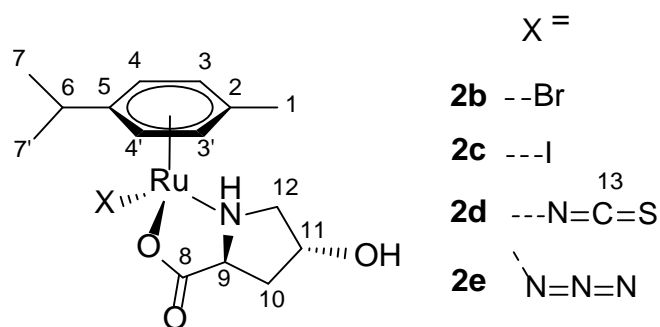
5.64, 5.60 (d, $^3J_{\text{HH}} = 5.9$ Hz, 2H, C³H + C⁴H); 5.54–5.49 (m), 5.43 (d, $^3J_{\text{HH}} = 5.8$ Hz) (2H, C^{3'}H + C^{4'}H), 3.59 (t, $J = 8.4$ Hz, 1H, C¹²H), 3.18–3.11 (m, 1H, C¹²H'), 2.92 (dd, $^3J_{\text{HH}} = 10.3, 6.6$ Hz, 1H, C⁹H), 2.17 (s, 3H, C¹H), 1.33–1.29 (m) (C⁷H + C^{7'}H). Isomer ratio = 4 (¹H NMR, CD₃OD). ¹³C{¹H} NMR (CD₃OD): $\delta/\text{ppm} = 186.1$ (C⁸), 101.7 (C⁵), 96.6 (C²); 85.1, 83.9 (C³ + C⁴); 80.9, 80.7 (C^{3'} + C^{4'}); 63.1 (C⁹), 58.1 (C¹²), 32.0 (C⁶), 30.1 (C¹⁰), 27.7 (C¹¹); 22.8, 22.6 (C⁷ + C^{7'}); 18.0 (C¹). ¹⁴N NMR (CD₃OD): $\delta/\text{ppm} = -130$ ($\Delta\nu_{1/2} = 110$ Hz), -241 ($\Delta\nu_{1/2} = 150$ Hz) (N₃).

[Ru(κ N-NO₂)(κ^2 N,*O*-Pro)(η^6 -*p*-cymene)], **1f.** Prepared from [RuCl₂(η^6 -*p*-cymene)]₂ (38 mg, 0.062 mmol), ProH (15 mg, 0.13 mmol) and NaNO₂ (9.0 mg, 0.13 mmol) according to general procedure **B**. Yellow solid. Yield: 37 mg, 75%. Soluble in water, MeOH, CH₂Cl₂, insoluble in Et₂O. X-ray quality crystals of **1f** were obtained from a MeOH-acetone solution layered with Et₂O and settled aside at -20 °C. Anal. Calcd. For C₁₅H₂₂N₂O₄Ru: C, 45.56; H, 5.61; N, 7.08. Found: C, 45.45; H, 5.56; N, 7.12. IR (solid state): $\tilde{\nu}/\text{cm}^{-1} = 3432\text{w-br}$ (ν_{NH}), 3195w-br, 3065w-br, 2962m, 2927w-sh, 2873w, 2810w, 1828w-br, 1622s ($\nu_{\text{asym}}\text{CO}_2$), 1509w, 1568w-sh, 1541m, 1365s ($\nu_{\text{sym}}\text{CO}_2 + \nu_{\text{asym}}\text{NO}_2$), 1304s ($\nu_{\text{sym}}\text{NO}_2$), 1219m-sh, 1200m-sh, 1118m, 1092m, 1054m, 1035m, 1006w, 983w, 933m, 859m, 818s (δNO_2), 804m-sh, 777w, 697w, 673w. ¹H NMR (CD₃OD, major isomer): $\delta/\text{ppm} = 5.84$ (d, $^3J_{\text{HH}} = 6.0$ Hz, 1H, C⁴H), 5.67 (s, 2H, C^{3'}H + C^{4'}H), 5.46 (d, $^3J_{\text{HH}} = 5.9$ Hz, 1H, C³H), 4.03–3.96 (m, 1H, C¹²H), 3.38 (t, $^3J_{\text{HH}} = 8.4$ Hz, 1H, C⁹H), 3.28–3.19 (m, 1H, C¹²H'), 2.79 (hept, $^3J_{\text{HH}} = 6.9$ Hz, 1H, C⁶H), 2.22–2.18 (m, 1H, C¹⁰H), 2.17 (s, 3H, C¹H), 2.02–1.94 (m, 1H, C¹¹H), 1.87–1.71 (m, 2H, C¹⁰H' + C¹¹H'); 1.32, 1.26 (d, $^3J_{\text{HH}} = 6.8$ Hz, 6H, C⁷H + C^{7'}H). ¹H NMR (CD₃OD, minor isomer): $\delta/\text{ppm} = 5.55$ –5.52 (m, 2H, C⁴H + C^{4'}H); 5.40, 5.36 (d, $^3J_{\text{HH}} = 6.0$ Hz, 2H, C³H + C^{3'}H), 3.73–3.63 (m, 1H, C¹²H), 2.95–2.85 (m, 2H, C⁹H + C¹²H'), 2.65–2.53 (m, 1H, C⁶H), 2.24 (s, 3H, C¹H); 1.42, 1.30 (d, $^3J_{\text{HH}} = 6.9$ Hz, 6H, C⁷H + C^{7'}H). Isomer ratio = 5 (¹H NMR, CD₃OD). ¹³C{¹H} NMR (CD₃OD): $\delta/\text{ppm} = 186.1$ (C⁸), 105.4 (C⁵), 101.4 (C²); 89.0, 86.6 (C³ + C⁴); 84.3, 83.6 (C^{3'} + C^{4'}); 81.7 (C^{4'}), 63.8 (C⁹), 59.3 (C¹²), 32.3 (C⁶), 30.6 (C¹⁰), 27.8 (C¹¹); 22.8, 22.5 (C⁷ + C^{7'}); 18.2 (C¹). ¹⁴N NMR (CD₃OD): $\delta/\text{ppm} = -349$ ($\Delta\nu_{1/2} = 2 \cdot 10^3$ Hz, NO₂).

[Ru(CN)(κ^2N,O -Pro)(η^6 -*p*-cymene)], **1g.** Prepared from [RuCl₂(η^6 -*p*-cymene)]₂ (41 mg, 0.067 mmol), ProH (17 mg, 0.15 mmol) and KCN (10 mg, 0.15 mmol) according to general procedure **B**. Contaminated glassware was treated with bleach, in order to remove traces of cyanide residues. Yellow-orange, slightly hygroscopic solid. Yield: 41 mg, 81%. Soluble in acetone, CH₂Cl₂, insoluble in Et₂O. IR (solid state): $\tilde{\nu}/\text{cm}^{-1}$ = 3425w-br (νNH), 3128w-br, 3062w-br, 2961m, 2928w-sh, 2873m, 2801w, 2105m (νCN), 1622s-br (ν_{asym}CO₂), 1536w, 1505w, 1468m, 1447m, 1374m-sh, 1357s (ν_{sym}CO₂), 1315m, 1298m, 1261m-sh, 1199m, 1159w, 1114w, 1079m, 1055m, 1042m-sh, 1009w, 980w, 928m, 863m, 803m, 770w, 723w, 692w, 673w. ¹H NMR (CD₃OD, major isomer): δ/ppm = 5.86, 5.74, 5.69, 5.49 (d, ³J_{HH} = 5.9 Hz, 4H, C³H + C^{3'}H + C⁴H + C^{4'}H); 3.83 (dd, ²J_{HH} = 11.2 Hz, ³J_{HH} = 6.9 Hz, 1H, C¹²H), 3.53 (dd, ³J_{HH} = 9.6, 5.0 Hz, 1H, C⁹H), 2.94 (td, ²J_{HH} = 11.4 Hz, ³J_{HH} = 5.3 Hz, 2H, C¹²H'), 2.75 (hept, ³J_{HH} = 7.0 Hz, 1H, C⁶H), 2.16 (s, 3H, C¹H); 2.14–2.08, 1.99–1.86, 1.84–1.69 (m, 4H, C¹⁰H + C¹¹H); 1.29 (d, ³J_{HH} = 6.9 Hz, 6H, C⁷H + C^{7'}H). ¹H NMR (CD₃OD, minor isomer): δ/ppm = 5.92, 5.88, 5.61, 5.52 (d, ³J_{HH} = 6.3 Hz, 4H, C³H + C^{3'}H + C⁴H + C^{4'}H); 4.02–3.94 (m, 1H, C¹²H). Isomer ratio ≈ 8 (¹H NMR, CD₃OD). ¹³C{¹H} NMR (CD₃OD): δ/ppm = 185.2 (C⁸), 138.9 (C¹³), 106.8 (C⁵), 103.2 (C²); 89.7, 89.0, 83.52, 83.48 (C³ + C^{3'} + C⁴ + C^{4'}); 64.7 (C⁹), 59.6 (C¹²), 32.6 (C⁶), 29.6 (C¹⁰), 27.6 (C¹¹); 23.0, 22.7 (C⁷ + C^{7'}); 18.6 (C¹).

[RuX(κ^2N,O -Hyp)(η^6 -*p*-cymene)], **2b-e (Chart 3).**

Chart 3. Structures of **2b-e** (numbering refers to C atoms).



Compounds **2b-e** were prepared according to general procedures **A** and **B**, as described for the related L-proline derivatives, using *trans*-4-hydroxy-L-proline (HypH). Compound **2d** required a modification in the work-up (see below).

[RuBr(κ^2N,O -Hyp)(η^6 -*p*-cymene)], 2b. Prepared from [RuBr₂(η^6 -*p*-cymene)]₂ (53 mg, 0.067 mmol) and HypH (18 mg, 0.14 mmol) according to general procedure **A**. Yellow-orange solid. Yield: 50 mg, 84%. Soluble in DMF, MeOH, CH₂Cl₂, acetone, H₂O, insoluble in Et₂O. X-ray quality crystals of **2b** were obtained from a DMF solution layered with Et₂O and settled aside at -20 °C. Anal. Calcd. For C₁₅H₂₂BrNO₃Ru: C, 40.46; H, 4.98; N, 3.15. Found: C, 40.35; H, 5.03; N, 3.20. IR solid state: $\tilde{\nu}/\text{cm}^{-1}$ = 3295w-br (ν_{NH}), 3204m-sh (ν_{OH}), 3061w, 3050w-sh, 2962m-br 2928w, 2872w, 1601s-br (ν_{asymCO_2}), 1565s-sh, 1497w, 1470w, 1434m, 1376s-br (ν_{symCO_2}), 1362s-br, 1307m, 1277w, 1264w, 1201m, 1134w, 1113w, 1072m-sh, 1053s (ν_{COH}), 1002w-sh, 956w, 927m, 865m, 855m-sh, 804w, 764w, 731w, 698w, 669w. ¹H NMR (CD₃OD, major isomer): δ/ppm = 5.71 (d, ³J_{HH} = 5.6 Hz, 1H), 5.68–5.65, 5.57–5.52 (m) (4H, C³H + C^{3'}H + C⁴H + C^{4'}H), 4.40 (m, 1H, C¹¹H), 3.88 (d, ²J_{HH} = 12.0 Hz, 1H, C¹²H), 3.70 (t, ³J_{HH} = 8.7 Hz, 1H, C⁹H), 3.25 (d, ²J_{HH} = 12.1 Hz, 1H, C¹²H'), 2.86 (hept, ³J_{HH} = 6.9 Hz, 2H, C⁶H), 2.19 (s, 3H, C¹H); 2.16–2.07, 2.02–1.88 (m, 2H, C¹⁰H); 1.34, 1.29 (d, ³J_{HH} = 6.8 Hz, 6H, C⁷H + C^{7'}H). ¹H NMR (CD₃OD, minor isomer): δ/ppm = 4.25 (m, 1H, C¹¹H), 3.19 (d, ²J_{HH} = 12.6 Hz, 1H, C¹²H), 2.16 (s, 3H, C¹H), 1.32–1.29 (C⁷H + C^{7'}H). Isomer ratio = 4 (¹H NMR, CD₃OD). ¹³C{¹H} NMR (CD₃OD, major isomer): δ/ppm = 186.0 (C⁸), 102.3 (C⁵), 97.2 (C²); 85.2, 84.2 (C³ + C⁴); 80.6, 80.4 (C^{3'} + C^{4'}); 72.6 (C¹¹), 65.3 (C¹²), 62.8 (C⁹), 39.3 (C¹⁰), 32.3 (C⁶); 23.0, 22.3 (C⁷ + C^{7'}), 18.5 (C¹). ¹³C{¹H} NMR (CD₃OD, minor isomer): δ/ppm = 103.1 (C⁵), 96.1 (C²); 84.0, 83.5, 81.4, 80.8 (C³ + C^{3'} + C⁴ + C^{4'}); 73.4 (C¹¹), 63.0 (C¹²), 39.4 (C¹⁰), 32.3 (C⁶), 22.7, 22.6 (C⁷ + C^{7'}).

[RuI(κ^2N,O -Hyp)(η^6 -*p*-cymene)], 2c. Prepared from [RuI₂(η^6 -*p*-cymene)]₂ (57 mg, 0.058 mmol) and HypH (15 mg, 0.11 mmol) according to general procedure **A**. Orange solid. Yield: 51 mg, 89%. Soluble in MeOH, EtOH, CH₂Cl₂, less soluble in H₂O and insoluble in Et₂O. X-ray quality crystals of **2c** were obtained from an EtOH solution layered with Et₂O and settled aside at -20 °C. Anal. Calcd. For

C₁₅H₂₂INO₃Ru: C, 36.59; H, 4.50; N, 2.85. Found: C, 36.51; H, 4.42; N, 2.89. IR (solid state): $\tilde{\nu}/\text{cm}^{-1}$ = 3340m-br (νNH), 3218m (νOH), 3043w, 2958m-br, 2911m, 2873w, 1634s-br ($\nu_{\text{asym}}\text{CO}_2$), 1536w, 1496w, 1472m, 1447m, 1416m, 1385m-sh ($\nu_{\text{sym}}\text{CO}_2$), 1360m-sh, 1344s-br, 1327s, 1298m, 1287m, 1259w, 1216w, 1204w, 1172w, 1116m, 1089w, 1054s (νCOH), 1042m-sh, 1020w, 1000m, 963w, 923m, 865m, 804m, 733w, 698w, 670w. ¹H NMR (CD₃OD, major isomer): δ/ppm = 5.85 (d, ³J_{HH} = 5.9 Hz, 1H, C⁴H), 5.72–5.68 (m, 2H, C³H + C⁴H), 5.50 (d, ³J_{HH} = 5.9 Hz, 1H, C³H), 4.44 (m, 1H, C¹¹H), 3.90 (d, ²J_{HH} = 12.1, 1H, C¹²H), 3.77 (t, ³J_{HH} = 8.8, 1H, C⁹H), 3.3* (m, C¹²H'), 2.89 (hept, ³J_{HH} = 6.6 Hz, 1H, C⁶H), 2.21 (s, 3H, C¹H); 2.15–2.04, 2.04–1.91 (m, 2H, C¹⁰H); 2.02 (dd, ³J_{HH} = 8.4, ²J_{HH} = 4.9 Hz, 1H, C¹⁰H); 1.34, 1.29 (d, ³J_{HH} = 6.9 Hz, 6H, C⁷H + C^{7'}H). *Covered by CD₂H resonance. ¹H NMR (CD₃OD, minor isomer): δ/ppm = 5.88, 5.77, 5.71, 5.59 (d, ³J_{HH} = 5.8 Hz, 4H, C³H + C^{3'}H + C⁴H + C^{4'}H), 4.22 (m, 1H, C¹¹H), 3.95–3.82 (m, 2H, C⁹H + C¹²H), 2.18 (s, 3H, C¹H), 1.31–1.29 (C⁷H + C^{7'}H). Isomer ratio = 5 (¹H NMR, CD₃OD). ¹³C{¹H} NMR (CD₃OD, major isomer): δ/ppm = 185.9 (C⁸), 102.4 (C⁵), 97.8 (C²); 85.6, 84.9 (C³ + C⁴); 80.61, 80.59 (C^{3'} + C^{4'}); 72.6 (C¹¹), 66.0 (C¹²), 63.8 (C⁹), 39.0 (C¹⁰), 32.6 (C⁶); 23.4, 22.3 (C⁷ + C^{7'}); 19.0 (C¹). ¹³C{¹H} NMR (CD₃OD, minor isomer): δ/ppm = 84.5, 84.1, 81.6, 80.5 (C³ + C^{3'} + C⁴ + C^{4'}); 73.4 (C¹¹), 66.1 (C¹²), 63.3 (C⁹), 38.8 (C¹⁰), 32.5 (C⁶); 23.0, 22.6 (C⁷ + C^{7'}); 18.9 (C¹).

[Ru($\kappa\text{N-NCS})(\kappa^2\text{N},\text{O-Hyp})(\eta^6\text{-}p\text{-cymene})]$, **2d.** Prepared from [Ru(SCN)₂($\eta^6\text{-}p\text{-cymene})$]₂ (32 mg, 0.046 mmol) and HypH (12 mg, 0.092 mmol) according to general procedure **A**, with a slight modification in the work-up. The crude was dissolved in the minimum amount of MeOH, then carefully diluted with CH₂Cl₂ and the resulting suspension was filtered over celite. The yellow filtrate was dried under vacuum and suspended in CH₂Cl₂ overnight, to ensure complete separation from NaSCN. Follows as per general procedure. Ochre yellow-orange solid, stored under dry N₂. Yield: 30 mg, 77%. Compound **2d** is soluble in acetone, MeCN, MeOH, less soluble in CH₂Cl₂, insoluble in Et₂O. X-ray quality crystals of **2d** were obtained from a MeCN solution layered with Et₂O and settled aside at –20 °C. Anal. Calcd. For C₁₆H₂₂N₂O₃RuS: C, 45.38; H, 5.24; N, 6.61; S, 7.57. Found: C, 45.49; H, 5.16; N,

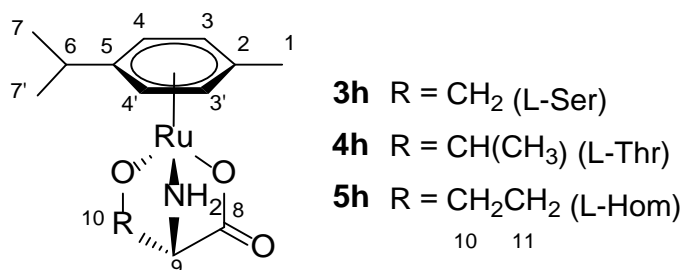
6.57; S, 7.63. IR (solid state): $\tilde{\nu}/\text{cm}^{-1} = 3378\text{m-br (vNH)}, 3180\text{m-br (vOH)}, 3060\text{m-sh}, 2963\text{m}, 2925\text{m}, 2872\text{m}, 2815\text{w}; 2089\text{s}, 2050\text{m-sh (SCN)}; 1606\text{s (v}_{\text{asym}}\text{CO}_2), 1501\text{w}, 1469\text{m}, 1437\text{m}, 1365\text{s (v}_{\text{sym}}\text{CO}_2), 1326\text{m}, 1307\text{m}, 1277\text{w-sh}, 1217\text{w}, 1201\text{w}, 1128-1118\text{w}, 1055\text{m (vCOH)}, 999\text{w}, 956\text{w}, 930\text{m}, 874\text{m}, 817\text{w}, 804\text{m}, 764\text{w}, 699\text{w}, 670\text{w}.$ $^1\text{H NMR (CD}_3\text{OD): } \delta/\text{ppm} = 7.89-7.79, 6.04-5.93 \text{ (m, 0.6H, NH)}; 5.82, 5.78, 5.73, 5.68 \text{ (d, } ^3J_{\text{HH}} = 5.9 \text{ Hz)}, 5.66-5.61 \text{ (m)}, 5.55, 5.49 \text{ (d, } ^3J_{\text{HH}} = 5.9 \text{ Hz)} \text{ (4H, C}^3\text{H + C}^{3'}\text{H + C}^4\text{H + C}^{4'}\text{H)}; 4.43-4.35 \text{ (m, 1H, C}^{11}\text{H)}, 3.96-3.82 \text{ (m, 1H, C}^{12}\text{H)}; 3.56-3.48, 3.30-3.25 \text{ (m, 1H, C}^9\text{H)}; 3.20-3.07 \text{ (m, 1H, C}^{12}\text{H}') \text{; 2.80 (hept, } ^3J_{\text{HH}} = 7.0 \text{ Hz, C}^6\text{H)}; 2.18, 2.16 \text{ (s, 3H, C}^1\text{H)}; 2.15-1.98, 1.86-1.75 \text{ (m, 2H, C}^{10}\text{H)}; 1.35 \text{ (d, } ^3J_{\text{HH}} = 6.9 \text{ Hz)}, 1.33-1.29 \text{ (m) (6H, C}^7\text{H + C}^{7'}\text{H)}.$ Isomer ratio = 1 ($^1\text{H NMR, CD}_3\text{OD}$). $^{13}\text{C}\{^1\text{H}\} \text{ NMR (CD}_3\text{OD): } \delta/\text{ppm} = 185.6, 185.3 \text{ (C}^8\text{)}; 138.8, 138.7 \text{ (C}^{13}\text{)}; 104.0, 103.8 \text{ (C}^5\text{)}; 98.9, 98.7 \text{ (C}^2\text{)}; 85.0, 84.4, 84.1, 83.3 \text{ (C}^3 + \text{C}^4\text{)}; 82.5, 82.4, 82.0, 81.9 \text{ (C}^{3'} + \text{C}^{4'}\text{)}; 72.7, 72.6 \text{ (C}^{11}\text{)}; 65.3, 65.2 \text{ (C}^{12}\text{)}; 62.9, 62.6 \text{ (C}^9\text{)}; 39.7, 39.1 \text{ (C}^{10}\text{)}; 32.4, 32.3 \text{ (C}^6\text{)}; 22.78, 22.76, 22.6, 22.5 \text{ (C}^7 + \text{C}^{7'}\text{)}; 18.3 \text{ (C}^1\text{)}.$ $^{14}\text{N NMR (CD}_3\text{OD): } \delta/\text{ppm} = -264 \text{ (}\Delta\nu_{1/2} = 4 \cdot 10^2 \text{ Hz, SCN)}.$

[Ru(N₃)(κ^2 N,*O*-Hyp)(η^6 -*p*-cymene)], 2e. Prepared from [RuCl₂(η^6 -*p*-cymene)]₂ (34 mg, 0.056 mmol), HypH (15 mg, 0.11 mmol) and NaN₃ (9.0 mg, 0.14 mmol) according to general procedure **B**. Yellow-orange solid. Yield: 36 mg, 79%. Soluble in MeOH, CH₂Cl₂, H₂O, insoluble in Et₂O. X-ray quality crystals of **2e** were obtained from a MeOH/acetone solution layered with Et₂O and settled aside at -20 °C. Anal. Calcd. For C₁₅H₂₂N₄O₃Ru: C, 44.22; H, 5.44; N, 13.75. Found: C, 44.16; H, 5.48; N, 13.79. IR (solid state): $\tilde{\nu}/\text{cm}^{-1} = 3350\text{w-br (vNH)}, 3290\text{w-br (vOH)}, 3065\text{w}, 2961\text{m}, 2928\text{w}, 2871\text{w}, 2025\text{s-br (vN}_3\text{)}, 1600\text{s-br (v}_{\text{asym}}\text{CO}_2), 1500\text{w}, 1470\text{m}, 1441\text{m}, 1362\text{m-br (v}_{\text{sym}}\text{CO}_2), 1303\text{m}, 1283\text{m}, 1200\text{w}, 1177\text{w}, 1134\text{w}, 1116\text{w}, 1084\text{w-sh}, 1055\text{m (vCOH)}, 1019\text{m}, 1004\text{m}, 956\text{w}, 931\text{m}, 908\text{w}, 868\text{m}, 802\text{m}, 764\text{w}, 698\text{w}, 667\text{w}.$ $^1\text{H NMR (CD}_3\text{OD, major isomer): } \delta/\text{ppm} = 5.69, 5.57 \text{ (d, } ^3J_{\text{HH}} = 5.9 \text{ Hz, 2H, C}^3\text{H + C}^4\text{H)}; 5.52, 5.41 \text{ (d, } ^3J_{\text{HH}} = 5.9 \text{ Hz, 2H, C}^{3'}\text{H + C}^{4'}\text{H)}; 4.37 \text{ (t, } ^3J_{\text{HH}} = 3.6 \text{ Hz, 1H, C}^{11}\text{H)}, 3.78 \text{ (dd, } ^2J_{\text{HH}} = 12.3 \text{ Hz, } ^3J_{\text{HH}} = 1.7 \text{ Hz, 1H, C}^{12}\text{H)}, 3.47 \text{ (t, } ^3J_{\text{HH}} = 8.7 \text{ Hz, 1H, C}^9\text{H)}, 3.18 \text{ (dd, } ^2J_{\text{HH}} = 12.2 \text{ Hz, } ^3J_{\text{HH}} = 3.1 \text{ Hz, 1H, C}^{12}\text{H}') \text{; 2.92-2.74 (m, 1H, C}^6\text{H)}, 2.21 \text{ (s, 3H, C}^1\text{H)}; 2.16-2.09, 1.99-1.91 \text{ (m, 2H, C}^{10}\text{H)}; 1.36 \text{ (d, } ^3J_{\text{HH}} = 6.9 \text{ Hz)}, 1.34-1.30 \text{ (m) (6H, C}^7\text{H + C}^{7'}\text{H')}.$ $^1\text{H NMR (CD}_3\text{OD, minor isomer):$

$\delta/\text{ppm} = 5.66, 5.61$ (d, $^3J_{\text{HH}} = 6.0$ Hz, 2H, $\text{C}^3\text{H} + \text{C}^4\text{H}$); $5.52, 5.44$ (d, $^3J_{\text{HH}} = 5.7$ Hz, 2H, $\text{C}^{3'}\text{H} + \text{C}^{4'}\text{H}$); 4.29 (s-br, 1H, C^{11}H), 3.86 (dd, $^2J_{\text{HH}} = 11.2$ Hz, $^3J_{\text{HH}} = 7.6$ Hz, 1H, C^{12}H), 3.09 (s-br, 2H, $\text{C}^9\text{H} + \text{C}^{12}\text{H}'$), 2.17 (s, 3H, C^1H), 2.05 (dd, $J = 12.8, 7.7$ Hz, 1H, C^{10}H), $1.76\text{--}1.67$ (m, 1H, $\text{C}^{10}\text{H}'$). Isomer ratio = 1.5 (^1H NMR CD_3OD). $^{13}\text{C}\{^1\text{H}\}$ NMR (CD_3OD , major isomer): $\delta/\text{ppm} = 185.9$ (C^8), 101.8 (C^5), 96.8 (C^2); $85.1, 83.7$ ($\text{C}^3 + \text{C}^4$); $81.0, 80.5$ ($\text{C}^{3'} + \text{C}^{4'}$); 72.6 (C^{11}), 64.9 (C^{12}), 62.0 (C^9), 39.6 (C^{10}), 32.0 (C^6); $22.9, 22.6$ ($\text{C}^7 + \text{C}^{7'}$); 18.0 (C^1). $^{13}\text{C}\{^1\text{H}\}$ NMR (CD_3OD , minor isomer): $\delta/\text{ppm} = 83.5, 81.5$ ($\text{C}^3 + \text{C}^4$); 72.9 (C^{11}), 62.8 (C^{12}), 60.8 (C^9), 39.4 (C^{10}). ^{14}N NMR (CD_3OD): $\delta/\text{ppm} = -130$ ($\Delta\nu_{1/2} = 120$ Hz), -239 ($\Delta\nu_{1/2} = 170$ Hz) (N_3).

[Ru($\kappa^3\text{N}, \text{O}, \text{O}'\text{-O}_2\text{CCH}(\text{NH}_2)(\text{R})\text{O}$)($\eta^6\text{-p-cymene}$)], 3-5h (Chart 4).

Chart 4. Structure of **3-5h** (numbering refers to C atoms).



General procedure. A suspension of $[\text{RuCl}_2(\eta^6\text{-p-cymene})]_2$ (45-80 mg) in deaerated $^t\text{PrOH}$ (5 mL) was heated at 75°C under nitrogen. Solutions of the selected α -amino acid (2 eq) in H_2O (0.3 mL) and 1.0 M NaOH (4-5 eq) were added dropwise to the hot, stirred mixture. Progressive colour change from orange to yellow and formation of a colourless precipitate (NaCl) were observed. After 2 hours, volatiles were removed under vacuum (40°C) and the residue was triturated in MeCN. The suspension was filtered through a celite pad and the filtrate solution was dried under vacuum. The resulting yellow, slightly hygroscopic solid was washed with Et_2O , dried under vacuum (40°C) and stored under N_2 .

[Ru($\kappa^3\text{N}, \text{O}, \text{O}'\text{-Ser}$)($\eta^6\text{-p-cymene}$)], 3h. Prepared from $[\text{RuCl}_2(\eta^6\text{-p-cymene})]_2$ (85 mg, 0.14 mmol), L-Serine (29 mg, 0.28 mmol) and 1.0 M NaOH (0.60 mL, 0.60 mmol) according to the general procedure. Yield: 77 mg, 81%. Soluble in water, MeOH, CH_2Cl_2 , CHCl_3 , moderately soluble in MeCN,

insoluble in Et₂O. Anal. Calcd. for C₁₃H₁₉NO₃Ru: C, 46.15; H, 5.66; N, 4.14. Found: C, 46.03; H, 5.71; N, 4.09. IR (solid state): $\tilde{\nu}/\text{cm}^{-1}$ = 3392m-br, 3212m (νNH), 3114-3066m, 2960m, 2931m, 2870m, 2827m, 1618s-br (ν_{asym}CO₂), 1528w, 1497w, 1470m, 1449w-sh, 1385s (ν_{sym}CO₂), 1319w, 1295m, 1198w-sh, 1155w-br, 1119w, 1090w, 1055w-sh, 1029m, 1002w-sh, 924w, 875m, 803w. ¹H NMR (CD₃OD): δ/ppm = 5.53, 5.48 (d, ³J_{HH} = 5.8 Hz, 2H, C⁴H + C⁴H'); 5.30, 5.25 (d, ³J_{HH} = 5.8 Hz, 2H, C³H + C³H'); 3.29 (dd, ²J_{HH} = 8.7 Hz, ³J_{HH} = 2.4 Hz, 1H, C¹⁰H), 3.18* (d, ³J_{HH} = 2.2 Hz, 1H, C⁹H), 3.18* (d, ²J_{HH} = 8.9 Hz, 1H, C¹⁰H'), 2.82 (hept, ³J_{HH} = 6.9 Hz, 1H, C⁶H), 2.23 (s, 3H, C¹H); 1.32 (d + d, ³J_{HH} = 6.9 Hz, 6H, C⁷H + C⁷H'). *superimposed. ¹³C{¹H} NMR (CD₃OD): δ/ppm = 182.5 (C⁸), 101.3 (C⁵), 96.3 (C²); 81.1, 81.0 (C⁴ + C⁴'); 79.3, 79.2 (C³ + C³'); 65.9 (C¹⁰), 63.1 (C⁹), 32.4 (C⁶); 23.09, 23.05 (C⁷ + C⁷'); 18.5 (C¹).

[Ru(κ³N,O,O'-Thr)(η⁶-*p*-cymene)], 4h. Prepared from [RuCl₂(η⁶-*p*-cymene)]₂ (44 mg, 0.072 mmol), L-Threonine (18 mg, 0.15 mmol) and 1.0 M NaOH (0.40 mL, 0.40 mmol) according to the general procedure. Yield: 43 mg, 85%. Soluble in water, MeOH, less soluble in MeCN, CH₂Cl₃, CHCl₃, insoluble in Et₂O. Anal. Calcd. For C₁₄H₂₁NO₃Ru: C, 47.72; H, 6.01; N, 3.97. Found: C, 47.58; H, 6.02; N, 4.00. IR (solid state): $\tilde{\nu}/\text{cm}^{-1}$ = 3261w, 3232w, 3200w (νNH); 3098m, 3062w-sh, 2964m, 2927m, 2891w, 2873w, 2840w, 1634m-sh (ν_{asym}CO₂), 1592s, 1519w, 1471w, 1457w, 1386s (ν_{sym}CO₂), 1350w, 1324w, 1298w, 1271w, 1187m, 1162m, 1106w, 1084w, 1049m, 1003w, 993m, 944m, 930w, 910w, 889w, 861m, 807w, 780w, 750w, 678w, 665w. ¹H NMR (CD₃OD): δ/ppm = 5.50, 5.47 (d, ³J_{HH} = 5.7 Hz, 2H, C⁴H + C⁴H'); 5.33, 5.28 (d, ³J_{HH} = 5.7 Hz, 2H, C³H + C³H'); 3.42 (q, ³J_{HH} = 6.3 Hz, 1H, C¹⁰H), 2.97 (s, 1H, C⁹H), 2.81 (hept, ³J_{HH} = 6.8 Hz, 1H, C⁶H), 2.21 (s, 3H, C¹H); 1.32, 1.31 (d, ³J_{HH} = 6.8 Hz, 6H, C⁷H + C⁷H'); 0.98 (d, ³J_{HH} = 6.3 Hz, 3H, C¹¹H). ¹³C{¹H} NMR (CD₃OD): δ/ppm = 183.4 (C⁸), 101.1 (C⁵), 95.4 (C²), 80.9 (C⁴); 80.3, 80.2 (C³ + C⁴'); 79.7 (C³'), 70.2 (C¹⁰), 66.8 (C⁹), 32.3 (C⁶); 23.2, 22.8 (C⁷ + C⁷'); 21.9 (C¹¹), 18.4 (C¹).

[Ru(κ³N,O,O'-Hom)(η⁶-*p*-cymene)], 5h. Prepared from [RuCl₂(η⁶-*p*-cymene)]₂ (50 mg, 0.082 mmol), L-Homoserine (21 mg, 0.18 mmol) and 1.0 M NaOH (0.45 mL, 0.45 mmol) according to the general

procedure. Yield: 45 mg, 79%. Soluble in water, MeOH, MeCN, insoluble in Et₂O. Anal. Calcd. for C₁₄H₂₁NO₃Ru: C, 47.71; H, 6.01; N, 3.97. Found: C, 47.61; H, 6.08; N, 3.92. IR (solid state): $\tilde{\nu}/\text{cm}^{-1}$ = 3420w-br, 3216w (νNH), 3133w, 3069w, 2959m, 2925m, 2868w, 2850w, 2823w, 1614s-br (ν_{asym}CO₂), 1469m, 1434m, 1383m-sh, 1367s (ν_{sym}CO₂), 1331m, 1309m, 1199w, 1156w, 1077m, 1055m, 1037sh, 1002w, 958w, 918w, 864w, 824w, 802w, 667w. ¹H NMR (CD₃OD): δ/ppm = 5.49 (d, ³J_{HH} = 5.7 Hz, 1H, C⁴H), 5.35 (d, ³J_{HH} = 5.7 Hz, 2H, C^{4'}H); 5.23, 5.06 (d, ³J_{HH} = 5.8 Hz, 1H; C³H + C^{3'}H); 3.53–3.43 (m, 2H, C⁹H + C¹¹H), 3.15–3.06 (m, 1H, C¹¹H'), 2.86 (hept, ³J_{HH} = 7.0 Hz, 1H, C⁶H), 2.18 (s, 3H, 3H, C¹H), 1.64–1.52 (m, 2H, C¹⁰H), 1.34 (t, ³J_{HH} = 6.8 Hz, 6H, C⁷H + C^{7'}H). ¹³C{¹H} NMR (CD₃OD): δ/ppm = 184.6 (C⁸), 101.9 (C⁵), 95.8 (C²), 83.2 (C⁴), 82.6 (C^{4'}), 79.81, 79.76 (C³ + C^{3'}); 61.1 (C¹¹), 56.5 (C⁹), 35.0 (C¹⁰), 32.2 (C⁶), 23.2, 22.8 (C⁷ + C^{7'}), 18.1 (C¹).

Alternative procedure(s) and serendipitous isolation of [Ru₂(μ-H)₂(μ-Cl)(η⁶-*p*-cymene)₂]Cl. A suspension of [RuCl₂(η⁶-*p*-cymene)]₂ (50–80 mg), NaHCO₂ (2–8 eq) and the selected α-amino acid (2 eq) in MeOH or water (10 mL) was heated at reflux for 2 to 5 h. The resulting mixture (yellow solution + colourless precipitate) was treated as described above. Under these conditions, compounds **3-5h** were invariably obtained in a mixture with the intermediate (unreacted) chloro complexes **3-5a** and hydride by-products, in variable amounts. During an attempt to prepare **3h**, an orange-red oily residue was obtained at the end of the reaction. The residue was suspended in CH₂Cl₂ and moved on top of a silica column (h 5, d 2.3 cm). A violet band was collected by elution with neat MeOH. Volatiles were removed under vacuum (40 °C), affording a violet solid. ¹H NMR data are consistent with [Ru₂(μ-H)₂(μ-Cl)(η⁶-*p*-cymene)₂]Cl,²² along with traces of **3h**. ¹H NMR (CD₃OD): δ/ppm = 5.83 (d), 5.67 (d) (³J_{HH} = 5.7 Hz, 4H, C₆H₄); 2.68 (hept, ³J_{HH} = 6.9 Hz, 1H, CHMe₂), 2.31 (s, 3H, CMe), 1.33 (d, ³J_{HH} = 6.8 Hz, 6H, CHMe₂), –13.27 (s, 1H, Ru-H).

[RuCl(κ²N,*O*-SerH)(η⁶-*p*-cymene)], 3a and [Ru(κ²N,*O*-Ser)(κP-PTA)(η⁶-*p*-cymene)]Cl, [3i]Cl (Chart 5).

necessary; otherwise [**3i**]Cl is inseparable from NaCl or KCl co-products. Soluble in water, DMSO, poorly soluble in MeOH; almost insoluble in all other common organic solvents (CH₂Cl₂, acetone, MeCN, CH₃NO₂, Et₂O). Anal. Calcd. For C₁₉H₃₂ClN₄O₃PRu: C, 42.90; H, 6.06; N, 10.53. Found: C, 42.81; H, 6.12; N, 10.42. IR (solid state): $\tilde{\nu}/\text{cm}^{-1}$ = 3360m-br (νOH), 3220m-br(νNH), 3056m, 2960m, 2934m, 2875m, 1623s (ν_{asym}CO₂), 1504w, 1469w, 1445w, 1415w, 1376m (ν_{sym}CO₂), 1352m, 1290-1280m, 1241m, 1199w, 1161w, 1099m, 1055m, 1040m, 1013m, 970s, 946s, 899m, 866w, 800m, 740m. ¹H NMR (CD₃OD): δ/ppm = 6.32, 5.31 (m-br, 1H, NH); 6.14 (d), 6.11–6.01 (m), 5.91 (d), 5.88 (d) (³J_{HH} ≈ 5.9 Hz, 4H, C³H + C⁴H); 4.70–4.59 (m, 6H, C¹¹H); 4.41–4.27 (m, 6H, C¹²H); 4.01–3.92 (m, H, C¹⁰H); 3.86, 3.72 (dd, ²J_{HH} = 10.8 Hz, ³J_{HH} = 2.6 Hz, 1H, C¹⁰H'); 3.58–3.52, 3.21–3.16 (m, 1H, C⁹H); 2.63 (hept, ³J_{HH} = 6.5 Hz, 1H, C⁶H); 2.07, 2.06 (s, 3H, C¹H); 1.27–1.20 (m, 6H, C⁷H). Isomer ratio = 1.3 (¹H NMR CD₃OD, 24 h). ¹³C{¹H} NMR (D₂O): δ/ppm = 182.8, 181.3 (C⁸); 107.5, 107.2 (C⁵); 102.4, 102.3 (C²); 90.1 (d, ³J_{CP} = 5.8 Hz), 89.4 (d, ³J_{CP} = 5.8 Hz), 88.3, 87.9, 87.5 (d, ³J_{CP} = 2.9 Hz), 87.1 (d, ³J_{HH} = 3.1 Hz), 86.6, 86.1 (C³H + C⁴H); 70.8, 70.8 (C¹¹); 62.2, 61.7 (C¹⁰), 60.3–59.9 (m, C⁹); 49.9 (d), 49.3 (d) (³J_{HP} = 15 Hz, C¹²), 30.8 (C⁶); 22.0, 21.96, 21.91, 21.8 (C⁷), 17.4 (C¹). ³¹P{¹H} NMR (CD₃OD): δ/ppm = – 37.4, – 37.8. ³⁵Cl NMR (D₂O): δ/ppm = 1.86 (Δν_{1/2} = 35 Hz, Cl[–]).

3. X-ray crystallography

Crystal data and collection details for [Ru(N₃)₂(η⁶-*p*-cymene)]₂ (**Ru-N3**), **1f**, **2b**, **2c**, **2d** and **2e** are reported in Table 5. Data were recorded on a Bruker APEX II diffractometer equipped with PHOTON2 detector using Mo–Kα radiation. Data were corrected for Lorentz polarization and absorption effects (empirical absorption correction SADABS).⁴⁹ The structures were solved by direct methods and refined by full-matrix least-squares based on all data using *F*².⁵⁰ Hydrogen atoms were fixed at calculated positions and refined by a riding model except the N-bonded and O-bonded hydrogens which were located in the Fourier map and refined isotropically. All non-hydrogen atoms were refined with anisotropic displacement parameters. The crystals of **2b** are twinned and they have been refined

using the TWIN 1 0 0 0 -1 0 0 0 -1 -4 line in SHELXL and three batch factors which refined as 0.35(3), 0.07(3) and 0.06(3).

Table 5. Crystal data and measurement details for **Ru-N3**, **1f**, **2b**, **2c**, **2d** and **2e**.

	Ru-N3	1f	2b	2c	2d	2e
Formula	C ₂₀ H ₂₈ N ₁₂ Ru ₂	C ₁₅ H ₂₂ N ₂ O ₄ Ru	C ₁₅ H ₂₂ BrNO ₃ Ru	C ₁₅ H ₂₂ N ₄ O ₃ Ru	C ₁₆ H ₂₂ N ₂ O ₃ RuS	C ₁₅ H ₂₂ INO ₃ Ru
FW	638.68	395.41	445.31	407.43	423.48	492.30
T, K	100(2)	100(2)	100(2)	100(2)	100(2)	100(2)
λ , Å	0.71073	0.71073	0.71073	0.71073	0.71073	0.71073
Crystal system	Triclinic	Orthorhombic	Monoclinic	Orthorhombic	Monoclinic	Orthorhombic
Space group	$P\bar{1}$	$P2_12_12_1$	$P2_1$	$P2_12_12_1$	$P2_1$	$P2_12_12_1$
<i>a</i> , Å	8.0847(4)	6.8530(4)	6.8687(15)	7.1174(3)	5.9679(9)	10.4798(7)
<i>b</i> , Å	8.2571(5)	10.6283(6)	23.288(5)	9.9265(4)	9.9595(15))	11.7879(8)
<i>c</i> , Å	9.7821(5)	21.8157(13)	10.082(2)	23.0044(10)	14.192(2)	13.2428(10)
α , °	83.3520(10)	90	90	90	90	90
β , °	85.0850(10)	90	91.108(9)	90	90.801(5)	90
γ , °	77.2420(10)	90	90	90	90	90
Cell Volume, Å ³	631.39(6)	1588.96(16)	1612.4(6)	1625.28(12)	843.4(2)	1635.9(2)
Z	1	4	4	4	2	4
<i>D</i> _c , g·cm ⁻³	1.680	1.653	1.834	1.665	1.668	1.999
μ , mm ⁻¹	1.229	1.006	3.459	0.985	1.069	2.854
F(000)	320	808	888	832	432	960
Crystal size, mm	0.22 x 0.16 x 0.14	0.19 x 0.16 x 0.12	0.19 x 0.16 x 0.11	0.16 x 0.13 x 0.10	0.14 x 0.13 x 0.09	0.19 x 0.16 x 0.12
θ limits, °	2.100-27.999	1.867-26.999	2.020-25.005	1.770-26.994	2.498-25.000	2.313-25.975
Reflections collected	9239	24410	10106	33705	13243	21646
Independent reflections	3024 [<i>R</i> _{int} = 0.0177]	3472 [<i>R</i> _{int} = 0.0228]	5346 [<i>R</i> _{int} = 0.0781]	3539 [<i>R</i> _{int} = 0.0611]	2953 [<i>R</i> _{int} = 0.1494]	3216 [<i>R</i> _{int} = 0.0372]
Data / restraints /parameters	3024 / 0 / 157	2472 / 0 / 203	5346 / 472 / 384	3539 / 0 / 212	2953 / 1 / 212	3216 / 145 / 193
Goodness on fit on F ²	1.162	1.157	1.074	1.123	1.018	1.395
<i>R</i> ₁ (<i>I</i> > 2 σ (<i>I</i>))	0.0177	0.0141	0.0723	0.0150	0.0418	0.0480
<i>wR</i> ₂ (all data)	0.0457	0.0352	0.2044	0.0374	0.0910	0.1324
Absolute structure parameter	-	0.01(3)	0.06(3)	-0.011(7)	0.06(4)	0.04(9)
Largest diff. peak and hole, e Å ⁻³	0.325 / -0.7074	0.400 / -0.0352	2.825 / -2.798	0.304 / -0.385	1.393 / -0.636	1.218 / -1.886

4. Speciation, solubility and stability in aqueous solutions, partition coefficient.

Speciation in water and cell culture medium. *NMR measurements.* Freshly-prepared solutions of Ru compounds ($\approx 1.2 \cdot 10^{-2}$ M) in D₂O (**1a-c**, **2a-c**, **1-2e**) or in D₂O/CD₃OD 5:2 v/v (**1-2d**) were filtered over celite and analysed by ¹H and ³⁵Cl/⁸¹Br/¹²⁷I NMR spectroscopy (A). Therefore, an excess of the

corresponding alkali metal (pseudo)halide was added (NaCl for **1-2a**, NaBr for **1-2b**, NaI for **1-2c**, KSCN for **1-2d**, NaN₃ for **1-2e**) and the ¹H NMR spectrum was repeated (**B**). In a second set of experiments, the same solutions were treated with AgNO₃ (0.11 M in D₂O, 50 μL, 1.0 equivalent) and stirred for 15'. The mixtures were filtered over celite and analysed by ¹H NMR spectroscopy (**C**); for compounds **1-2d** and **1-2e**, ¹H NMR spectrum was repeated after 24 h at room temperature (**D**). In a final set of experiments, freshly-prepared solutions of Ru compounds (c ≈ 1.2·10⁻² M) in DMEM-d (**1a-c**, **2a-c**, **1-2e**) or in DMEM-d/CD₃OD 5:2 v/v (**1-2d**) were filtered over celite and analysed by ¹H and NMR spectroscopy (**E**).

NMR data analysis. Comparison of ¹H NMR spectra of solutions **A**, **B**, **C**, **D** allowed unambiguous assignment of resonances to the neutral (pseudo)halido (**1a-e**, **2a-e**, starting material) and the cationic aquo [**1-2w**]⁺ complexes. The relative % of (pseudo)halido and aquo complexes in the D₂O solution (**A**) were calculated by integration of suitable non-overlapping signals related to the same CH_x group in the two species (Table 1). NMR data for the tested compounds are reported in the Supporting Information; ¹H NMR signals are referenced to D₂O [δ/ppm = 4.79]; spectra were aligned to the D₂O solution (**A**) to compensate for ionic strength effects on chemical shift.

Conductivity and pH measurements. Conductivity and pH of freshly prepared solutions of **1a-e** and **2a-e** in deionized water (≈ 2·10⁻³ M) were measured (Table 1). Solutions were then kept at room temperature (21 ± 1 °C) for 24 h; minimal variations in pH and conductivity were observed.

Solubility in water (D₂O). The selected Ru compound was suspended in a D₂O solution (0.2 mL) containing dimethyl sulfone (Me₂SO₂; 4.3·10⁻³ M) and stirred at 21 °C for 3 h. The resulting saturated solution was diluted with D₂O (0.7 mL total volume) filtered over celite and analysed by ¹H NMR spectroscopy (delay time = 3 s; number of scans = 20). The concentration (= solubility) was calculated by the relative integral with respect to Me₂SO₂ as internal standard⁵¹ [δ/ppm = 3.14 (s, 6H)] (Table 2).

Octanol-water partition coefficient (Log P_{ow}). Partition coefficients (P_{ow}), defined as P_{ow} = c_{org}/c_{aq}, where c_{org} and c_{aq} are the molar concentrations of the selected compound in the n-octanol and aqueous

phases, respectively, were determined by the shake-flask method and UV-Vis measurements, according to a previously described procedure.⁵² All operations were carried out at $21 \pm 1^\circ\text{C}$. Stock solutions of all compounds were prepared in octanol-saturated water. The wavelength of the maximum absorption of each compound (320–380 nm range) was used for UV-Vis quantitation. The procedure was repeated three times for each sample (from the same stock solution); results are given as mean \pm standard deviation (Table 2).

Stability in D₂O (or D₂O/CD₃OD). The selected Ru compound (*ca.* 4 mg) was dissolved in a D₂O solution containing Me₂SO₂ ($4.3 \cdot 10^{-3}$ M, 0.7 mL). Compound **1d** was first dissolved in CD₃OD (0.2 mL) then diluted with the D₂O/Me₂SO₂ solution (0.5 mL). The yellow solution ($c_{\text{Ru}} \approx 8 \cdot 10^{-3}$ M) was stirred for 30 minutes then filtered over celite and analysed by ¹H and ³¹P{¹H} NMR (delay time = 3 s; number of scans = 20). Next, the solution was heated at 37 °C for 48 h and NMR analyses were repeated. The residual amount of starting material in solution (% with respect to the initial spectrum) was calculated by the relative integral with respect to Me₂SO₂ as internal standard⁵¹ (Table 2). NMR data for the tested compounds are reported in the Supporting Information; ¹H NMR signals are referenced to Me₂SO₂ as in pure D₂O [$\delta/\text{ppm} = 3.14$].

Stability in cell culture medium (DMEM-d or DMEM-d/CD₃OD). Powdered Dulbecco's Modified Eagle Medium (DMEM; 1000 mg/L glucose and L-glutamine, without sodium bicarbonate and phenol red; D2902 - Sigma Aldrich) was dissolved in D₂O (10 mg/mL), according to the manufacturer's instructions. The solution of deuterated cell culture medium ("DMEM-d") was treated with Me₂SO₂ ($3.7 \cdot 10^{-3}$ M) and NaH₂PO₄ / Na₂HPO₄ (0.10 M, $\text{pD} = 7.4^{53}$), then stored at 4 °C under N₂. Solutions of Ru compounds in DMEM-d (or DMEM-d/CD₃OD 5:2 v/v for **1d**) were prepared, treated and analysed by ¹H NMR as previously described (Table 2; thermal treatment time: 24 h).

5. Cytotoxicity

The human ovarian carcinoma cell lines (A2780CisR and A2780) were purchased from the European Collection of Cell Cultures (ECACC). The human embryonic kidney 293T (HEK-293T) cell line was kindly provided by the biological screening facility (EPFL, Switzerland). Penicillin streptomycin, RPMI 1640 GlutaMAX (where RPMI = Roswell Park Memorial Institute), and DMEM GlutaMAX media (where DMEM = Dulbecco's modified Eagle medium) were obtained from Life Technologies, and fetal bovine serum (FBS) was obtained from Merck. The cells were cultured in RPMI 1640 GlutaMAX (A2780, A2780cisR) and DMEM GlutaMAX (HEK-293T) media containing 10% heat-inactivated FBS and 1% penicillin streptomycin at 37 °C and CO₂ (5%). Cisplatin was routinely added to the culture medium of the A2780cisR cell line to obtain a final concentration of 2 µM, that is needed to preserve the resistance against cisplatin. The MTT assay was used to determinate the cytotoxicity of the compounds. 100 µL of the cell suspension were seeded in flat-bottomed 96-well at approximately 4300 cells/well and preincubated for 24 h at 37 °C. Stock solutions of the compounds were prepared in DMSO and were sequentially diluted to give a final compound concentration range (0–100 µM). Cisplatin and RAPTA-C were used as positive (0–100 µM) and negative (200µM) controls respectively. The compounds were added in quadruplets to the preincubated 96-well plates in 20 µL aliquots to which 80 µL of medium were added to have a final volume of 200 µL at the final concentrations mentioned above. The plates were then incubated for a further 72 h. MTT (20 µL, 5 mg/mL in Dulbecco's phosphate buffered saline) was added to the cells, and the plates were incubated for additional 4 h. The culture medium was delicately aspirated and the purple formazan crystals were dissolved in DMSO (100 µL/well). The absorbance of the resulting solutions, directly proportional to the number of surviving cells, was quantified at 590 nm using a SpectroMax M5e multimode microplate reader (SoftMax Pro software, version 6.2.2). The percentage of surviving cells was calculated (Graphpad prism software, version 9.2.0) from the absorbance of wells corresponding to the untreated control cells. The reported IC₅₀ values are based on the means from two independent experiments, each comprising four tests per concentration level.

6. Cellular uptake

The A2780 cells were seeded at a density of $2 \cdot 10^6$ cells in a 75 cm^2 flask and left to adhere overnight at 37°C . Flasks were prepared in triplicates for every compound (biological replicates from different T75 flasks). $50 \mu\text{L}$ of a 10 mM solution of every compound were added to the flasks to have a final $50 \mu\text{M}$ concentration in 10 mL of media. Plates were incubated for 5 hours; media was then disposed off and the flasks were washed 3 times with 10 mL of prewarmed DPBS solution. 3 mL of trypsin were added, followed by incubation for 10 minutes. 7 mL of medium were added and $10 \mu\text{L}$ of the cell suspension were sampled for cell counting. The 10 mL suspension was then centrifuged (790 RMP , $120 \times g$) for 10 minutes at room temperature and the supernatant was discarded. The determination of metal uptake in the A2780 cancer cell line was performed according to a well-established protocol,^{54,55} using a Varian 720-ES inductively coupled plasma atomic emission spectrometer (ICP-AES) equipped with a CETAC U5000 AT+ ultrasonic nebulizer, in order to increase the method sensitivity. Each sample of the cellular pellet was mineralized in a thermo-reactor at 80°C for 8 h with 2 mL of 50% v/v diluted aqua regia (HCl suprapure grade and HNO_3 suprapure grade in a 3:1 ratio) in Milli-Q water ($\geq 18 \text{ M}\Omega \cdot \text{cm}$). After that time, the samples were cooled down to room temperature and further diluted with 4 mL of ultrapure water ($\geq 18 \text{ M}\Omega \cdot \text{cm}$). All the samples were spiked with 1 ppm of Ge used as an internal standard and analysed. Calibration standards were prepared by gravimetric serial dilution from a commercial standard solution of Ru at 1000 mg L^{-1} . The wavelength used for Ru was 267.876 nm , whereas for Ge the line at 209.426 nm was used. The operating conditions were optimized to obtain maximum signal intensity and, between each sample, a rinsed solution of HCl suprapure grade and HNO_3 suprapure grade at a 3:1 ratio was used to avoid any “memory effect”. Finally, the ruthenium concentration was normalized to the cell number.

7. Binding studies with cytochrome c

The stock solution of Cytochrome c 10^{-3} M was prepared by dissolving the lyophilised and commercially available protein in $2 \cdot 10^{-3}$ M ammonium acetate solution (pH 6.8). The stock solutions $3 \cdot 10^{-2}$ M of the investigated Ru-based compounds were prepared by dissolving the samples in DMSO. For the ESI-MS experiments, each stock solution of the Ru complexes was mixed with an opportune aliquot of the protein stock solution in metal to protein ratio of 3:1 and diluted with ammonium acetate solution $2 \cdot 10^{-3}$ M (pH 6.8) to a protein concentration of 10^{-4} M (in these conditions the final percentage of DMSO was below 3%). The mixtures were incubated at 37 °C up to 72 h. After 24 and 72 h of incubation time, all solutions were sampled and diluted to a final protein concentration of 10^{-7} M using the ammonium acetate solution $2 \cdot 10^{-3}$ M (pH 6.8) and added with 0.1% v/v of formic acid just before the infusion in the mass spectrometer. The ESI mass spectra were acquired using a TripleTOF[®] 5600⁺ high-resolution mass spectrometer (Sciex, Framingham, MA, USA), equipped with a DuoSpray[®] interface operating with an ESI probe. All the ESI mass spectra were acquired through a direct infusion at 5 $\mu\text{L min}^{-1}$ flow rate. The general ESI source parameters optimized for Cyt c were as follows: positive polarity; ionspray voltage floating 5500 V, temperature (TEM) 25 °C, ion source gas 1 (GS1) 40 L min⁻¹; ion source gas 2 (GS2) 0 L min⁻¹; curtain gas (CUR) 25 L min⁻¹, declustering potential (DP) 150 V, collision energy (CE) 10 V, acquisition range 750-2500 m/z . For the acquisition, the Analyst TF 1.7.1 software (Sciex) was used and deconvolved spectra were obtained using the Bio Tool Kit v2.2 incorporated in the software PeakView[™] v.2.2 (Sciex).

Acknowledgements

We gratefully thank the University of Pisa (Fondi di Ateneo 2020 and PRA_2020_39) and the Swiss National Science Foundation for financial support.

Supporting Information Available (ESI).

Comparison of diastereomeric ratios and spectroscopic data. Solid-state IR and multinuclear NMR spectra of compounds. X-ray data: structure of **Ru-N3** and hydrogen bonding in **2b-2e**. Speciation and stability studies in water and in cell culture medium (^1H NMR data and spectra). Mass spectra following incubation with Cyt c. CCDC reference numbers 2104834(**Ru-N3**), 2104829(**1f**), 2104830(**2b**), 2104831(**2c**), 2104832(**2d**) and 2104833(**2e**) contain the supplementary crystallographic data for the X-ray studies reported in this paper. These data can be obtained free of charge at <https://www.ccdc.cam.ac.uk/structures/> or from the Cambridge Crystallographic Data Centre, 12, Union Road, Cambridge CB2 1EZ, UK; e-mail: deposit@ccdc.cam.ac.uk.

References

-
- ¹ (a) B. S. Murray and P. J. Dyson, *Curr. Opinion Chem. Biol.* 2020, **56**, 28–34; (b) P. Zhang and P. J. Sadler, *J. Organomet. Chem.* 2017, **839**, 5–14; (c) E. Boros, P. J. Dyson and G. Gasser, *Chem.* 2020, **6**, 41–60.
- ² (a) E. Alessio, *Eur. J. Inorg. Chem.* 2017, 1549–1560; (b) R. Trondl, P. Heffeter, C. R. Kowol, M. A. Jakupec, W. Berger and B. K. Keppler, *Chem. Sci.*, 2014, **5**, 2925.
- ³ (a) L. Zeng, P. Gupta, Y. Chen, E. Wang, L. Ji, H. Chao, Z.-S. Chen, *Chem. Soc. Rev.* 2017, **46**, 5771–5804; (b) E. J. Anthony, E. M. Bolitho, H. E. Bridgewater, O. W. L. Carter, J. M. Donnelly, C. Imberti, E. C. Lant, F. Lermite, R. J. Needham, M. Palau, P. J. Sadler, H. Shi, F.-X. Wang, W.-Y. Zhang and Z. Zhang, *Chem. Sci.*, 2020, **11**, 12888–12917; (c) B. S. Murray, M. V. Babak, C. G. Hartinger and P. J. Dyson, *Coord. Chem. Rev.* 2016, **306**, 2016, 86–114.
- ⁴ (a) H. Chen, J. A. Parkinson, R. E. Morris and P. J. Sadler, *J. Am. Chem. Soc.* 2003, **125**, 173–186; (b) C. Scolaro, C. G. Hartinger, C. S. Allardyce, B. K. Keppler and P. J. Dyson, *J. Inorg. Biochem.* 2008, **102**, 1743–1748.
- ⁵ S. M. Meier-Menches, C. Gerner, W. Berger, C. G. Hartinger and B. K. Keppler, *Chem. Soc. Rev.* 2018, **47**, 909–928.
- ⁶ Y. Zhang, W. Zheng, Q. Luo, Y. Zhao, E. Zhang, S. Liua and F. Wang, *Dalton Trans.*, 2015, **44**, 13100–13111.
- ⁷ (a) L. Biancalana, L. K. Batchelor, T. Funaioli, S. Zacchini, M. Bortoluzzi, G. Pampaloni, P. J. Dyson and F. Marchetti, *Inorg. Chem.* 2018, **57**, 11, 6669–6685; (b) L. K. Filak, S. Göschl, P. Heffeter, K. Ghannadzadeh Samper, A. E. Egger, M. A. Jakupec, B. K. Keppler, W. Berger and V. B. Arion, *Organometallics* 2013, **32**, 903–914; (c) O. A. Lenis-Rojas, M. P. Robalo, A. Isabel Tomaz, A. Carvalho, A. R. Fernandes, F. Marques, M. Folgueira, J. Yanez, D. Vazquez-Garcia, M. Lopez Torres, A. Fernandez and J. J. Fernandez, *Inorg. Chem.* 2018, **57**, 13150–13166.
- ⁸ S. J. Dougan, M. Melchart, A. Habtemariam, S. Parsons and P. J. Sadler, *Inorg. Chem.* 2006, **45**, 10882–10894.
- ⁹ (a) S. Parveen, M. Hanif, S. Movassaghi, M. P. Sullivan, M. Kubanik, M. Ashraf Shaheen, T. Söhnel, S. M. F. Jamieson and C. G. Hartinger, *Eur. J. Inorg. Chem.* 2017, **12**, 1721–1727; (b) L. Biancalana, G. Pampaloni, S. Zacchini and F. Marchetti, *J. Organomet. Chem.* 2018, **869**, 201–

- 211; (c) A. Kurzwernhart, W. Kandioller, S. Bachler, C. Bartel, S. Martic, M. Buczkowska, G. Mühlgassner, M. A. Jakupec, H.-B. Kraatz, P. J. Bednarski, V. B. Arion, D. Marko, B. K. Keppler and C. G. Hartinger, *J. Med. Chem.* 2012, **55**, 10512–10522; (d) J. P. Meszaros, H. Geisler, J. M. Poljarevic, A. Roller, M. S. Legina, M. Hejl, M. A. Jakupec, B. K. Keppler, W. Kandioller and E. A. Enyedy, *J. Organomet. Chem.* 2020, **907**, 121070.
- 10 (a) G. Ciancaleoni, I. Di Maio, D. Zuccaccia and A. Macchioni, *Organometallics* 2007, **26**, 489–496; (b) J. Yan, X. Lian Lu, J.-D. Lou, L. Zhang, P.-S. Nong, Y.-L. Feng, M. Gao and J.-J. Yang, *Synth. React. Inorg. Metal-Org. Nano-Met. Chem.*, 2011, **41**, 26–30; (c) R. Kramer, K. Polborn, H. Wanjek, I. Zahn and W. Beck, *Chem. Ber.* 1990, **123**, 767–778; (d) D. Carmona, F. J. Lahoz, R. Atencio, L. A. Oro, M. P. Lamata, F. Viguri, E. San José, C. Vega, J. Reyes, F. Joó and Á. Kathó, *Chem. Eur. J.* 1999, **5**, 1544–1564.
- 11 (a) D. Carmona, F. Viguri, M. P. Lamata, J. Ferrer, E. Bardají, F. J. Lahoz, P. García-Orduña and L. A. Oro, *Dalton Trans.*, 2012, **41**, 10298–10308; (b) K. S. Singh and P. H. Dixneuf, *ChemCatChem* 2013, **5**, 1313–1316; (c) W. Sun, C.-H. Ling, C.-M. Au, W.-Y. Yu, *Org. Lett.* 2021, **23**, 3310–3314.
- 12 (a) W. S. Sheldrick and S. Heeb, *Inorg. Chim. Acta*, 1990, **168**, 93–100; (b) A. Habtemariam, M. Melchart, R. Fernández, S. Parsons, I. D. H. Oswald, A. Parkin, F. P. A. Fabbiani, J. E. Davidson, A. Dawson, R. E. Aird, D. I. Jodrell and P. J. Sadler, *J. Med. Chem.* 2006, **49**, 6858–6868; (c) G. W. Karpin, J. S. Merola and J. O. Falkinham III, *Antimicrob. Agents Chemother.* 2013, **57**, 3434–3436; (d) Y.-H. Chang, W.-J. Leu, A. Datta, H.-C. Hsiao, C.-H. Lin, J.-H. Guh and J.-H. Huang, *Dalton Trans.*, 2015, **44**, 16107–16118.
- 13 L. Biancalana, I. Abdalghani, F. Chiellini, S. Zacchini, G. Pampaloni and M. Crucianelli, *Eur. J. Inorg. Chem.* 2018, 3041–3057.
- 14 (a) S. J. Dougan, A. Habtemariam, S. E. McHale, S. Parsons and P. J. Sadler, *Proc. Natl. Acad. Sci. USA* 2008, **33**, 11628–11633; (b) I. Romero-Canelon, L. Salassa and P. J. Sadler, *J. Med. Chem.* 2013, **56**, 1291–1300; (c) D. N. Pantic, S. Arandelovic, S. Radulovic, A. Roller, V. B. Arion and S. Grguric-Sipka, *J. Organomet. Chem.* 2016, **819**, 61–68; (d) E. Carrillo, S. Ramírez-Rivera, G. Bernal, G. Aquea, C. Tessini and F. A. Thomet, *Life Sciences* 2019, **217**, 193–201; (e) A. Mitrović, J. Kljun, I. Sosić, M. Ursić, A. Meden, S. Gobec, J. Kos and I. Turel, *Inorg. Chem.* 2019, **58**, 12334–12347; (f) K. Purkait, Ruturaj, A. Mukherjee and A. Gupta, *Inorg. Chem.* 2019, **58**, 15659–15670; (g) A. Mukherjee, S. Acharya, K. Purkait, K. Chakraborty, A. Bhattacharjee and

-
- A. Mukherjee, *Inorg. Chem.* 2020, **59**, 6581–6594; (h) E. Zanda, N. Busto, L. Biancalana, S. Zacchini, T. Biver, B. Garcia and F. Marchetti, *Chem.-Bio. Interact.* 2021, **344**, 109522.
- ¹⁵ (a) F. Wang, A. Habtemariam, E. P. L. van der Geer, R. Fernandez, M. Melchart, R. J. Deeth, R. Aird, S. Guichard, F. P. A. Fabbiani, P. Lozano-Casal, I. D. H. Oswald, D. I. Jodrell, S. Parsons and P. J. Sadler, *Proc. Natl. Acad. Sci. USA* 2005, **102**, 18269–18274; (b) M. Hanif, P. Schaaf, W. Kandioller, M. Hejl, M. A. Jakupec, A. Roller, B. K. Keppler and C. G. Hartinger, *Aust. J. Chem.* 2010, **63**, 1521–1528; (c) S. Betanzos-Lara, O. Novakova, R. J. Deeth, A. M. Pizarro, G. J. Clarkson, B. Liskova, V. Brabec, P. J. Sadler and A. Habtemariam, *J. Biol. Inorg. Chem.* 2012, **17**, 1033–1051; (d) M. Kubanik, H. Holtkamp, T. Söhnle, S. M. F. Jamieson and C. G. Hartinger, *Organometallics* 2015, **34**, 5658–5668; (e) D. Astudillo, A. Galdámez, M. E. Sanguinetti, J. Villena, F. A. Thomet, *Inorg. Chem. Commun.* 2017, **84**, 221–224; (f) S. Bhattacharyya, K. Purkait and A. Mukherjee, *Dalton Trans.*, 2017, **46**, 8539–8554; (h) J. Kljun, I. E. León, Š. Peršič, J. F. Cadavid-Vargas, S. B. Etcheverry, W. He, Y. Baid and I. Turel, *J. Inorg. Biochem.* 2018, **186**, 187–196; (g) A. Sarkar, S. Acharya, K. Khushvant, K. Purkait and A. Mukherjee, *Dalton Trans.* 2019, **48**, 7187–7197; (h) D. N. Pantić, L. E. Mihajlović-Lalić, S. Arandelović, S. Radulović, S. Grgurić-Šipka, *J. Coord. Chem.* 2019, **72**, 908–919; (i) S. Harringer, D. Wernitznig, N. Gajic, A. Diridl, D. Wenisch, M. Hejl, M. A. Jakupec, S. Theiner, G. Koellensperger, W. Kandioller and B. K. Keppler, *Dalton Trans.*, 2020, **49**, 15693–15711; (j) J. Arshad, K. K. H. Tong, S. Movassaghi, T. Söhnle, S. M. F. Jamieson, M. Hanif and C. G. Hartinger, *Molecules* 2021, **26**, 833; (k) F. Wang, A. Habtemariam, E. P. L. van der Geer, R. J. Deeth, R. Gould, S. Parsons and P. J. Sadler, *J. Biol. Inorg. Chem.* 2009, **14**, 1065–1076.
- ¹⁶ K. S. Singh and W. Kaminsky, *Polyhedron* 2014, **68**, 279–286.
- ¹⁷ D. Carmona, M. Pilar Lamata, F. Viguri, E. San José, A. Mendoza, F. J. Lahoz, P. García-Orduña, R. Atencio and L. A. Oro, *J. Organomet. Chem.* 2012, **717**, 152–163.
- ¹⁸ (a) A. C. da Silva, H. Piotrowski, P. Mayer, K. Polborn and K. Severin, *J. Chem. Soc., Dalton Trans.*, 2000, 2960–2963; (b) K. Mashima, K.-h. Kusano, T. Ohta, R. Noyori and H. Takaya, *J. Chem. Soc. Chem. Comm.*, 1989, 1208–1210; (c) M. G. Mendoza-Ferri, C. G. Hartinger, A. A. Nazarov, R. E. Eichinger, M. A. Jakupec, K. Severin and B. K. Keppler, *Organometallics* 2009, **28**, 6260–6265; (d) A. P. Walsh, W. W. Brennessel and W. D. Jones, *Inorg. Chim. Acta*, 2013, **407**, 131–138; (e) C. S. Allardyce, P. J. Dyson, D. J. Ellis, P. A. Salter and R. Scopelliti, *J. Organomet. Chem.* 2003, **668**, 35–42; (f) D. van der Waals, L. E. Heim, S. Vallazza, C. Gedig, J. Deska and M. H. G. Prechtel, *Chem. Eur. J.* 2016, **22**, 11568–11573.

- ¹⁹ R. A. Zelonka and M. C. Baird, *Can. J. Chem.* 1972, 3063-3072.
- ²⁰ (a) K. Sarjit Singh, V. Svitlyk, P. Devi and Y. Mozharivskyj, *Inorg. Chim. Acta* 2009, **362**, 5252–5258; (b) Y.-L. Liu, F.-H. Wu, T.-K. Duan and Q.-F. Zhang, *Chin. J. Struct. Chem.* 2009, **28**, 995–997; (c) Herein the compound was formed in solution and allowed to react *in situ*, without isolation: A. K. Renfrew, J. Karges, R. Scopelliti, F. D. Bobbink, P. Nowak-Sliwinska, G. Gasser and P. J. Dyson, *ChemBioChem* 2019, **20**, 2876–2882.
- ²¹ (a) J. Patalenszki, L. Bìro, A. Csaba Benyei, T. Radosova Muchova, J. Kasparkova and P. Buglyò, *RSC Adv.*, 2015, **5**, 8094-8107; (b) T. G. Scrase, M. J. O'Neill, A. J. Peel, P. W. Senior, P. D. Matthews, H. Shi, S. R. Boss and P. D. Barker, *Inorg. Chem.*, 2015, **54**, 3118–3124; (c) L. Bìró, E. Balogh and P. Buglyó, *J. Organomet. Chem.* 2013, **734**, 61-68; (d) F. A. Egbewande, L. E. H. Paul, B. Therrien and J. Furrer, *Eur. J. Inorg. Chem.* 2014, 1174–1184.
- ²² (a) M. A. Bennett, J. P. Ennett and K. I. Gell, *J. Organomet. Chem.* 1982, **233**, C17-C20; (b) M. A. Bennett and J. P. Ennett, *Organometallics* 1984, **3**, 1365-1374; (c) J. Chen, X. Chen, C. Zhu and J. Zhu, *J. Mol. Cat. A* 2014, **394**, 198–204.
- ²³ D. Carmona, A. Mendoza, F. J. Lahoz, L. A. Oro, M. Pilar Lamata and E. San Jose, *J. Organomet. Chem.* 1990, **396**, C17-C21.
- ²⁴ (a) H. D. Hansen, K. Maitra and J. H. Nelson, *Inorg. Chem.* 1999, **38**, 2150-2156; (b) N. Gul and J. H. Nelson *Organometallics* 1999, **18**, 709-725; (c) V. J. Catalano and T. J. Craig, *Polyhedron* 2000, **19**, 475–485; (d) D. A. Freedman, S. Kruger, C. Roosa and C. Wymer, *Inorg. Chem.* 2006, **45**, 9558–9568; (e) L. Vandenburg, M. R. Buck and D. A. Freedman *Inorg. Chem.* 2008, **47**, 9134-9136; (f) S. Dhara, M. A. Ansari and G. K. Lahiri, *Inorg. Chem.* 2019, **58**, 10991–10999; (g) R. Kumar, R. Ujjval and N. Thirupathi, *Eur. J. Inorg. Chem.* 2019, 3619–3628; (h) T. Mochida, S. Maekawa and R. Sumitani, *Inorg. Chem.* 2021, **60**, 12386–12391.
- ²⁵ J. A. Kargol, R. W. Crecely and J. L. Burmeister, *Inorg. Chem.* 1979, **18**, 2532-2535.
- ²⁶ K. Nakamoto, *Infrared and Raman Spectra of Inorganic and Coordination Compounds*, 5th ed; Wiley-Interscience: New York, 1997.
- ²⁷ $\nu(\text{CN}) = 2104 \text{ cm}^{-1}$ for $[\text{Ru}(\text{CN})(\eta^2\text{-(N}^i\text{Pr)PPh}(\text{NH}^i\text{Pr}))(\eta^6\text{-}p\text{-cymene})]$ to be compared with 2227–2237 cm^{-1} for $[\text{Ru}(\text{CN})(2,2'\text{-dipiridylamine})(\eta^6\text{-}p\text{-cymene})]\text{BF}_4$; (a) P. J. Bailey, K. J. Grant and S. Parsons, *Organometallics* 1998, **17**, 551-555; (b) P. Kumar, A. Kumar Singh, R. Pandey, P.-Z. Li, S. Kumar Singh, Q. Xu and D. Shankar Pandey, *J. Organomet. Chem.* 2010, **695**, 2205-2212.
- ²⁸ F. Marchetti an, G. Pampaloni, *Organometallic Complexes of Group 5 With π -Acidic Ligands* in *Comprehensive Organometallic Chemistry*, IV Edition. DOI: 10.1016/B978-0-12-820206-

7.00005-6. *Organometallic Complexes of Group 5 With π -Acidic Ligands, Reference Module in Chemistry, Molecular Sciences and Chemical Engineering*, Elsevier, 2021, DOI: 10.1016/B978-0-12-820206-7.00005-6.

- ²⁹ M. A. Hitchman and G. L. Rowbottom, *Coord Chem Rev.* 1982, **42**, 55-132.
- ³⁰ To be compared with 1391/1316 cm⁻¹ for [Ru(NO₂)(2,2'-bipyridine)(η^6 -*p*-cymene)]PF₆. See ref: 24d.
- ³¹ D. F. Dersnah and M. C. Baird, *J. Organomet. Chem.* 1977, **127**, C55–C58
- ³² D. Carmona, F. J. Lahoz, P. García-Orduña and L. A. Oro, *Organometallics* 2012, **31**, 3333–3345.
- ³³ Reference NMR data. ³⁵Cl NMR (NaCl, D₂O): δ /ppm = 5.1. ⁷⁹Br NMR (NaBr, D₂O): δ /ppm = 7.1. ¹²⁷I NMR (KI, D₂O): δ /ppm = 5.1. ¹⁴N NMR (KSCN, D₂O): δ /ppm = – 175.0. ¹⁴N NMR (NaN₃, D₂O): δ /ppm = – 133.1, – 281.7.
- ³⁴ A pK_a of 8.65 was previously determined for [Ru(O₂CCH₂NH₂)(H₂O)(η^6 -*p*-cymene)]⁺, see reference 12b. Based on this, and given the pH measurements, we can neglect the presence of hydroxo complexes in solution.
- ³⁵ A few additional resonances in the ¹H NMR spectra of freshly prepared solutions of 1-2c, that disappeared after 24 h at 37 °C. At this point, the ¹H NMR spectra of chloride, bromide and iodide complexes are totally superimposable.
- ³⁶ (a) L. E. H. Paul, B. Therrien and J. Furrer, *J. Biol. Inorg. Chem.* 2012 **17**, 1053–1062; (b) S. M. Meier, M. Hanif, W. Kandioller, B. K. Keppler and C. G. Hartinger, *J. Inorg. Biochem.*, 2012, **108**, 91-95.
- ³⁷ S. Dasari and P. B. Tchounwou, *Eur. J. Pharmacol.* 2014, **740**, 364–378.
- ³⁸ C. Scolaro, C. G. Hartinger, C. S. Allardyce, B. K. Keppler and P. J. Dyson, *J. Inorg. Biochem.*, 2008 **102**, 1743–1748.
- ³⁹ (a) G. Tamasi, A. Carpini, D. Valensin, L. Messori, A. Pratesi, F. Scaletti, M. Jakupec, B. Keppler and R. Cini, *Polyhedron*, 2014, **81**, 227–237; (b) T. Marzo, S.A. De Pascali, C. Gabbiani, F.P. Fanizzi, L. Messori, A. Pratesi, *Biometals*, 2017, **30**, 609-614; (c) L. Biancalana, A. Pratesi, F. Chiellini, S. Zacchini, T. Funaioli, C. Gabbiani, F. Marchetti, *New J. Chem.*, 2017, **41**, 14574-14588.
- ⁴⁰ (a) A. Pratesi, D. Cirri, L. Ciofi and L. Messori, *Inorg. Chem.*, 2018, **57**, 10507-10510; (b) G. Ferraro, A. Pratesi, L. Messori, A. Merlino, *Dalton Trans.*, 2020, **49**, 2412-2416.
- ⁴¹ (a) S. M. Meier, M. S. Novak, W. Kandioller, M. A. Jakupec, A. Roller, B. K. Keppler and C. G. Hartinger, *Dalton Trans.*, 2014, **43**, 9851–9855; (b) A. Casini, G. Mastrobuoni, W. H. Ang, C. Gabbiani, G. Pieraccini, G. Moneti, P. J. Dyson and L. Messori, *ChemMedChem*, 2007, **2**, 631–635.

-
- ⁴² From the MS spectrum alone, it is not possible to assert if the thiocyanate group is bound to ruthenium or somewhere else on the protein.
- ⁴³ M. A. Bennett and A. K. Smith, *J. Chem. Soc., Dalton Trans.* 1974, 233-241.
- ⁴⁴ C. S. Allardyce, P. J. Dyson, D. J. Ellis and S. L. Heath, *Chem. Commun.*, 2001, 1396–1397
- ⁴⁵ (a) R. K. Harris, E. D. Becker, S. M. Cabral De Menezes, R. Goodfellow and P. Granger, *Pure Appl. Chem.* 2001, **73**, 1795–1818; (b) G. R. Fulmer, A. J. M. Miller, N. H. Sherden, H. E. Gottlieb, A. Nudelman, B. M. Stoltz, J. E. Bercaw and K. I. Goldberg, *Organometallics* 2010, **29**, 2176–2179.
- ⁴⁶ W. Willker, D. Leibfritz, R. Kerssebaum and W. Bermel, *Magn. Reson. Chem.* 1993, **31**, 287-292.
- ⁴⁷ F. Menges, "Spectragryph - optical spectroscopy software", Version 1.2.16d, @ 2016-2020, <http://www.effemm2.de/spectragryph>.
- ⁴⁸ (a) W. J. Geary, *Coord. Chem. Rev.* 1971, **7**, 81-122.
- ⁴⁹ Sheldrick, G. M. SADABS-2008/1 - Bruker AXS Area Detector Scaling and Absorption Correction, Bruker AXS: Madison, Wisconsin, USA, 2008.
- ⁵⁰ Sheldrick, G. M. *Acta Crystallogr. C*, 2015, **71**, 3–8.
- ⁵¹ T. Rundlöf, M. Mathiasson, S. Bekiroglu, B. Hakkarainen, T. Bowden and T. Arvidsson. *J. Pharm. Biomed. Anal.* 2010, **52**, 645–651.
- ⁵² (a) OECD Guidelines for Testing of Chemicals. In OECD, Paris: 1995; Vol. 107; (b) J. C. Dearden and G. M. Bresnen, *Quant. Struct.-Act. Relat.* 1988, **7**, 133-144; (c) G. Agonigi, L. Biancalana, M. G. Lupo, M. Montopoli, N. Ferri, S. Zacchini, F. Binacchi, T. Biver, B. Campanella, G. Pampaloni, V. Zanotti and F. Marchetti, *Organometallics* 2020, **39**, 645-657.
- ⁵³ Calculated by the formula $pD = pH^* + 0.4$, where pH^* is the value measured for H₂O-calibrated pH-meter; (a) C. C. Westcott, pH Measurements; Academic Press: New York, 1978; (b) A. K. Covington, M. Paabo, R. A. Robinson and R. G. Bates. *Anal. Chem.* 1968, **40**, 700-706.
- ⁵⁴ G. Canil, S. Braccini, T. Marzo, L. Marchetti, A. Pratesi, T. Biver, T. Funaioli, F. Chiellini, J. D. Hoeschele and C. Gabbiani, *Dalton Trans.*, 2019, **48**, 10933-10944.
- ⁵⁵ S. Ciambellotti, A. Pratesi, M. Severi, G. Ferraro, E. Alessio, A. Merlino and L. Messori, *Dalton Trans.*, 2018, **47**, 11429-11437.